“Namuda”

gesture recognition for musical practice

three papers

by

Dr. Godfried-Willem Raes

post-doctoral researcher
Ghent University College & Logos Foundation

2010

This paper was presented in a preliminary draft version at the Thinktank session organised by IPEM, Ghent University, May 28th 2010, held on the premises of the Logos Foundation.

1

<Holosound ii2010>

a Doppler sonar and radar-based 3-D gesture measurement system

by

Dr. Godfried-Willem Raes

post-doctoral researcher
Ghent University College & Logos Foundation

2010

This technical note is a continuation of reports on many earlier designs for gesture sensing apparatus using both sonar and radar technologies. References to earlier designs are given in the reference section below. (1)

In this note we merely document the circuitry developed as an improvement of our 'Holosound' system, dating back to 1978 and updated in 2000. Hence the title, Holosound 2010. The design philosophy has been treated in depth in my writings on the 'Invisible Instrument'.

The main modifications to previous designs are:

1- the transducers in use here are omnidirectional wide-band sensors operating in the ultrasound range.
2- the new circuitry supports FM modulation of the base frequency, thus allowing distance measurement as well as a variety of analogue audio applications.
3- the circuitry can be used as such for audio installation projects and music theatre compositions, but for gesture analysis, the outputs should by sampled and further analysed by a computer. Unlike our previous designs, no special and expensive hardware is required here. Earlier systems invariably made use of National Instruments data acquisition hardware. This version requires up to six audio input channels on the PC, although the system can even be used with a common stereo input, be it restricted to two dimensions.
4- The signal/noise ratio has been improved by approx. 12 dB over earlier designs.
5- We have introduced the combined application of radar and sonar technology in order to achieve full gesture imaging, including positional information.

Receiver circuits for sonar (three are used in a tetrahedral set-up):

Although the highest possible Doppler frequencies for human bodies in movement using a 40 kHz carrier system are limited to less than 2.5 kHz (2), we have designed these receivers with an output bandwidth up to 16 kHz. This was done to allow frequency modulation schemes as well as the capture of ultrasonic components in audio input in general.

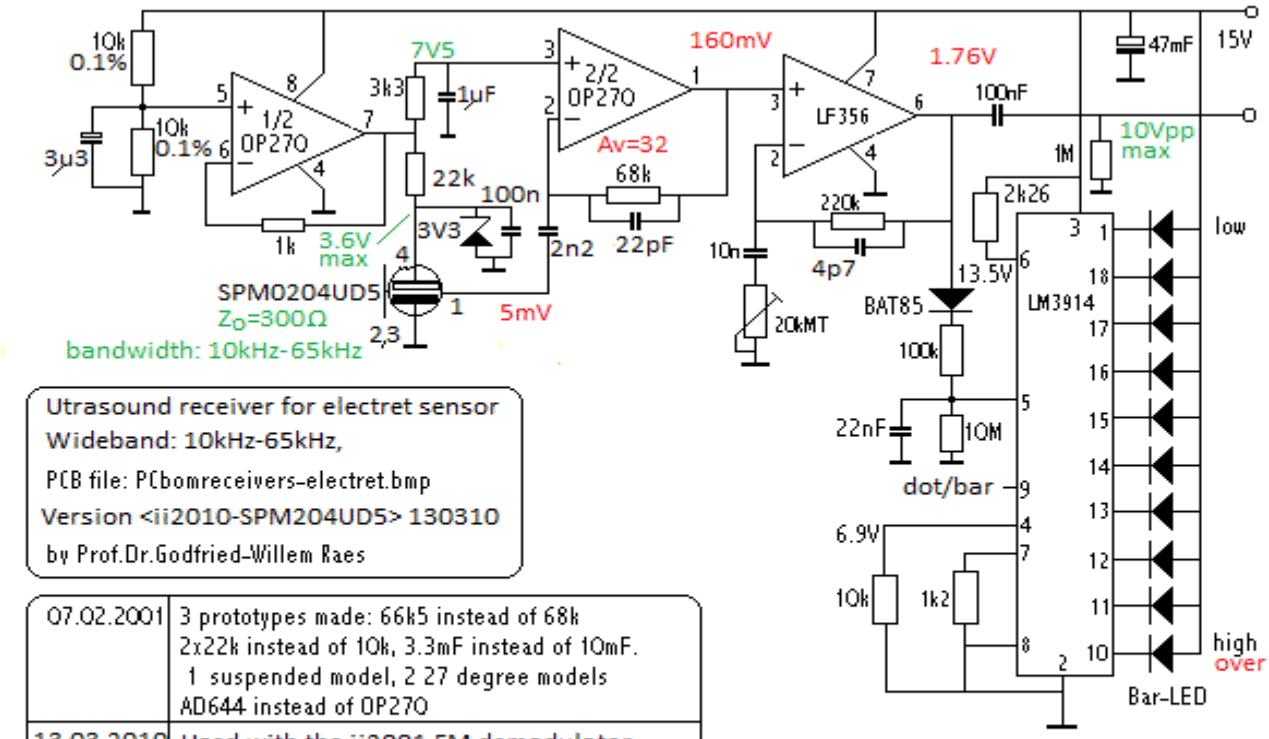

Utrasound receiver for electret sensor
Wideband: 10kHz-65kHz,
PCB file: PCbomreceivers-electret.bmp
Version <ii2010-SPM204UD5> 130310
by Prof.Dr.Godfried-Willem Raes

07.02.2001	3 prototypes made: 66k5 instead of 68k 2x22k instead of 10k, 3.3mF instead of 10mF. 1 suspended model, 2 27 degree models AD644 instead of OP270
13.03.2010	Used with the ii2001 FM demodulator S/N >55dB omnidirectional X-transducer: 20k, instead of 22k on mike Y-transducer: 22k Z-transducer: suspended

This became the sensor system of choice, after many circuits using the different transducers available on the market. On the picture shown below, one can see a circuit using a flexible transducer made by Pro Wave Electronics, type number 400FS080. We mention it, despite the lower signal noise ratio it offers, because it has interesting directional characteristics: 360 degree omnidirectional in the horizontal plane and +/-40 degrees vertical. It can be imagined as a doughnut shape, or in more scientific terms, a toroid. The bandwidth is limited to 4 kHz, centred around 40 kHz, wide enough to meet the requirements for FM modulation in distance estimation applications. (4)

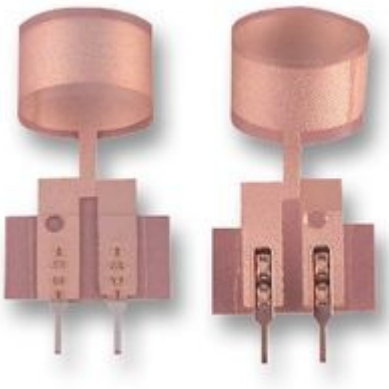

This type of transducer is also available with a centre frequency of 77 kHz (type 800FS049). The advantage of this higher frequency is that the Doppler signals are about an octave higher and thus frequency distribution calculation can be performed about two times faster. However, there are difficulties in building emitters with high enough sound pressure levels. We also have tried the Monacor electret capsule, type MCE2500, since its frequency response extends far into the

ultrasonic range. A suitable circuit is given in the notes (3). The obtainable S/N ratio is not as good as the SPM0204UD5 circuit, but it is considerably cheaper.

The sensor of choice used in our latest design, the SPM0204UD5 is an SMD MEMS component produced by Knowles Acoustics. Essential parameters and values are given in the circuit drawing. Note that the dot-driver is not a VU-meter but a tool to be used for alignment. It reflects the signal strength of the carrier wave. Reception will be best when any of the centre yellow LEDs are turned on. When the red LEDs turn on, the preamp is saturated and the signal clipped. When only the green LED lights up, the signal strength of the carrier wave is too low.

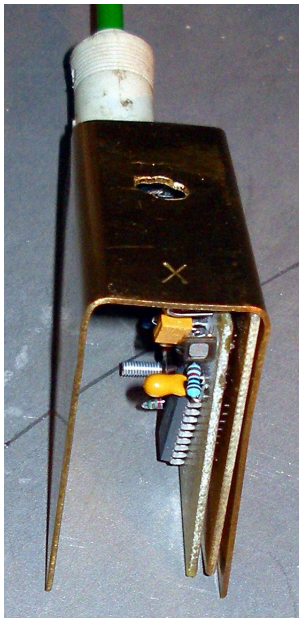

The X and Y receivers, fitted into their half-opened housing, look like this: Shielding of the circuit, although not shown in the picture, is very important, since the circuit is very sensitive to electromagnetic disturbances in its vicinity as commonly encountered with the proliferation of switch mode power supplies and motor controllers.

Analogue processor board:

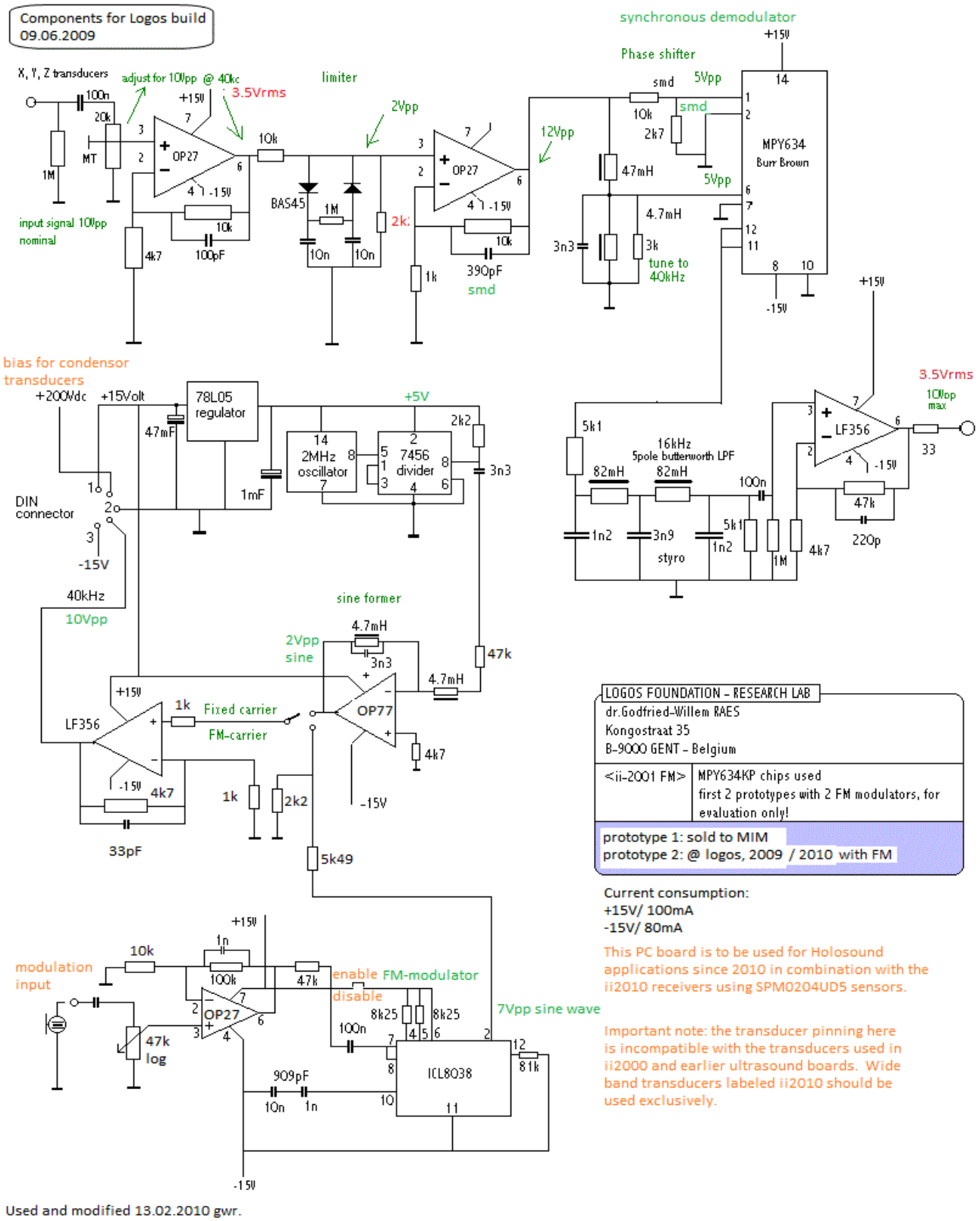

The outputs of this analogue computer can be sampled by normal audio cards. For full 3D gesture rendering, 3 channels of audio are required. To allow calculation of distances – requiring FM modulation of the carrier – one should use the fourth analogue channel to sample the modulation signal. (5) The circuit, three channels according to the circuit above, fits nicely on a Eurocard board (100x160 mm) and looks like this:

The limiter circuit with the two back to back diodes, is an old classic that will look familiar to anyone who ever worked with short wave radio circuitry. It's a very non-linear circuit giving good overload protection from large spikes and overloads. We provided for this because we wanted to use the circuit in combination with arbitrary sound sources extending into the ultrasonic range: bats, small bells, key-rattle, breaking glass, gas leaks etc. In a measurement system, this part of the circuit is inappropriate. It distorts amplitude measurement and thus body surface estimation. But if signal levels are kept below the forward voltage of the diodes, the circuit can very well be used for reliable amplitude calculations. To make the adjustment of the input levels easier, we have made a small analogue readout as follows:

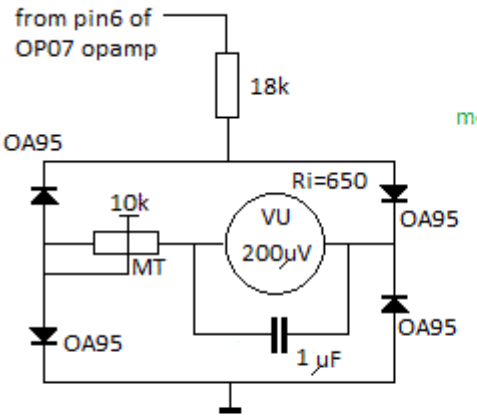

measurements with 40kHz sinewave signal

scale read out	Vrms	Vpp
+6dB	7.0V	20V
+3dB	5.34V	15V
0dB	4.0V	11.3V
-3dB	3.5V	10V
-6dB	2.7V	7.64V
-10dB	2.0V	5.66V
-20dB	1.19V	3.36V

ii2001: adjust for -3dB

last update: 30.04.2010

Three of these circuits are required and placed at the top of the analogue computing board. (12)

The demodulation takes place in a synchronous multiplier circuit. The advantage is that it makes an intrinsic high pass filter, cancelling out most Doppler frequencies related to extremely slow and involuntary movement. In the circuit used for <ii2000>, we demodulated against an ultra-stable carrier frequency reference and had to cope with very large, slowly moving DC offsets that had to

be removed in the processing software. The synchronous demodulator has a fixed phase angle relation between both of its inputs. Even sharper synchronous carrier separation can be obtained using 40 kHz crystals instead of the resonant LC circuit used here. We did not use crystals in this design however, because of the trouble we had with loss of carrier signal in frequency modulation schemes required for distance estimation.

A deficiency of the circuit presented is that the demodulation frequency is not easily tunable and with the given component values, it centres around 40 kHz, the most commonly used frequency in ultrasonic applications. It would be a benefit to be able to tune to arbitrary carrier frequencies in the range 20 kHz to 200 kHz.

An easy way to make the demodulation frequency independent is to feed to multipliers with the signals of a pair of transducers, i.e. xy, yx and zx. The output signals will now be the product of both inputs, and although the demodulated signals reflect the gesture very well, the maths involved to bring the data back to real world units (body surface and movement speed) becomes very complicated. (Raes, 1993) A proposal – using pure analogue circuitry – to solve this problem is given in this block diagram:

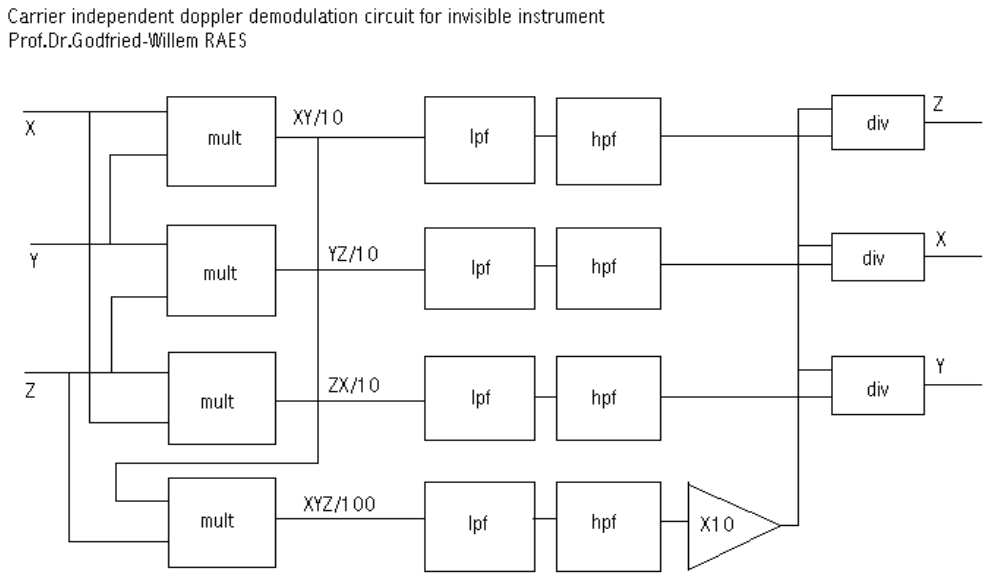

The multipliers can be either AD633 type (low cost analogue devices), or MPY632, AD534 etc. (expensive but a lot more precise). The dividers can be realized using the same chips in the appropriate divider configuration.

This idea can also be applied to individual receiver circuits, as we found out. In order to achieve this, each receiver is equipped with two sensors placed closely together. After pre-amplification, both signals are multiplied in an analogue multiplier, functioning here as a phase comparator. A 5th order low pass follows and some further amplification in order to get a sufficient signal level for sampling. This is the circuit as we tested it out:

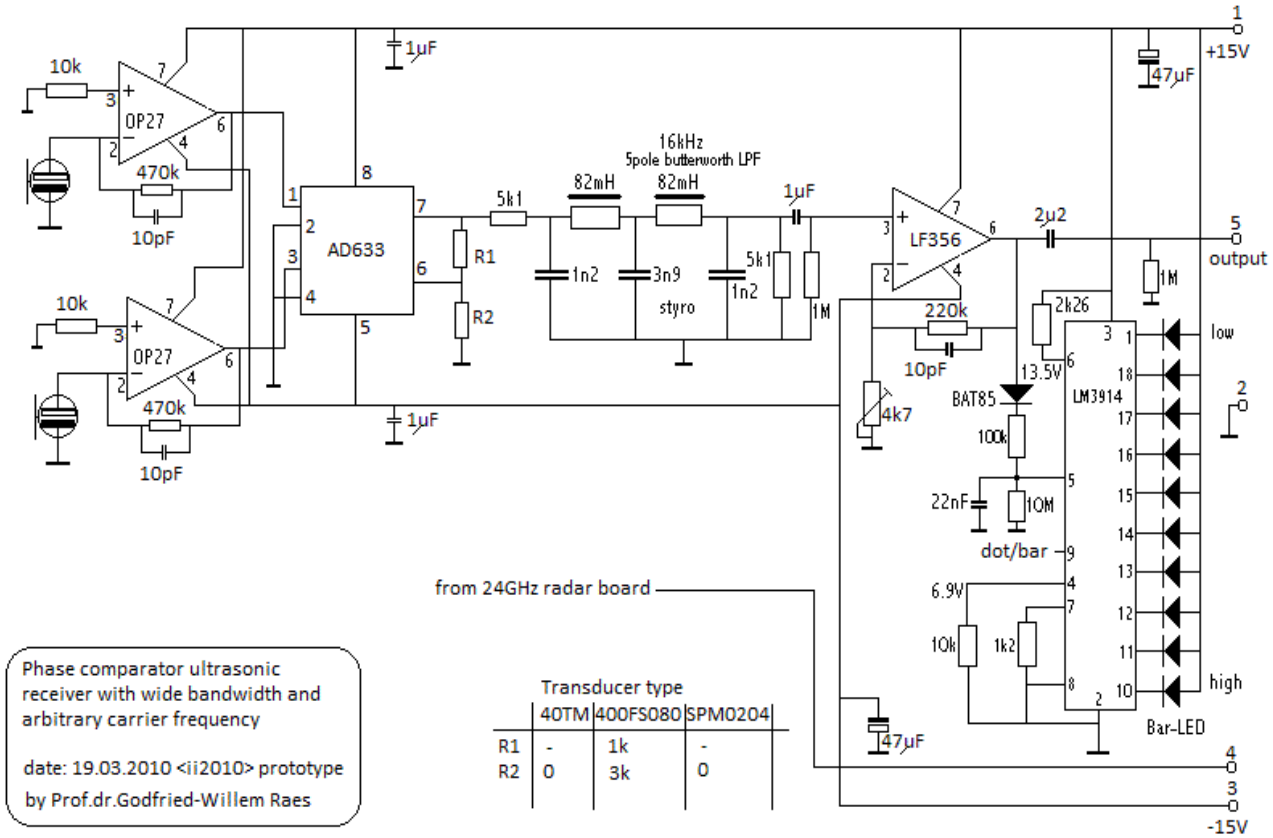

Performance of the circuit as a gesture-capturing device is good, but with the given components, the noise level (S/N ratio worst case, using 40TM transducers, 42 dB) is inferior to previous designs. This is mainly due to the 1 mV noise found on the output of the (cheap) multiplier. Another issue with this circuit is that it is very sensitive to large DC offset variations on the multiplier output in reaction to amplitude changes of the input signal. This could only be remedied by applying a phase shifter between both inputs as suggested in the application notes for the multiplier chip by Analog Devices. Unfortunately phase shifters only work well if the carrier frequency is constant and thus that solution would rule out the neat feature of this circuit, its carrier frequency independence. However, a phase shifter can also be realised mechanically:

When we consider only the sinusoidal ultrasonic carrier signal component, leaving the Doppler shifted components out of consideration, the multiplier operates as a squarer and thus, in the frequency domain, as a frequency doubler since we then have

$$U_o = \frac{(U_i \sin 2\Pi f t)^2}{10V} = \frac{U_i^2 (1 - \cos 4\Pi f t)}{20V}$$

This transfer equation shows a very high DC offset depending on input amplitude. To get rid of this, we can create a phase shift between the X and Y inputs of 90 degrees, and applying the textbook equation,

$$\cos a \sin a = \frac{\sin 2a}{2}$$

we can obtain:

$$U_o = \frac{1}{10V} U_i \sin(2\,\Pi f\,t + 45^o)\;\; U_i \sin(2\,\Pi f\,t - 45^o)$$

$$= \frac{U_i^2}{20V}(\sin 4\,\Pi f\,t)$$

Since both inputs in our application use individual sensors, this makes it possible to realize the phase shift without resorting to electronic networks. It is sufficient to place one of the transducers a quarter wavelength further back from the other. For a 40 kHz carrier, this means 2.125 mm, since a full wavelength corresponds to 8.5 mm.
By way of an aside: the circuit works very well for bat detection without any need for tuning, if used with the SPM0204 transducers.. If the output is to be sampled and the sampling rate in use is lower than 32kS/s, an extra low pass filter on the output becomes mandatory.
Although not discussed in full depth in this note (9), we have been using this board in combination with our 24 GHz microwave radar Doppler receivers. The radar board is piggy-back mounted on the ultrasound receiver board with the sensor aligned with the ultrasound sensors. This combined sensor offers the possibility to deduce the absolute distance to the moving body part, by measuring the time difference between both demodulated Doppler signals. Since ultrasound travels at the velocity of sound (340 m/s) and radar at the velocity of light, the time between the reception of the two signals allows us to deduce distance: s = 340.t Of course the resolution will be a function of the sampling rate. If the sampling rate is the common 44.1 kS/s, resolution will be 7.6 mm. Here is the full circuit for the combined sensor as we made it:

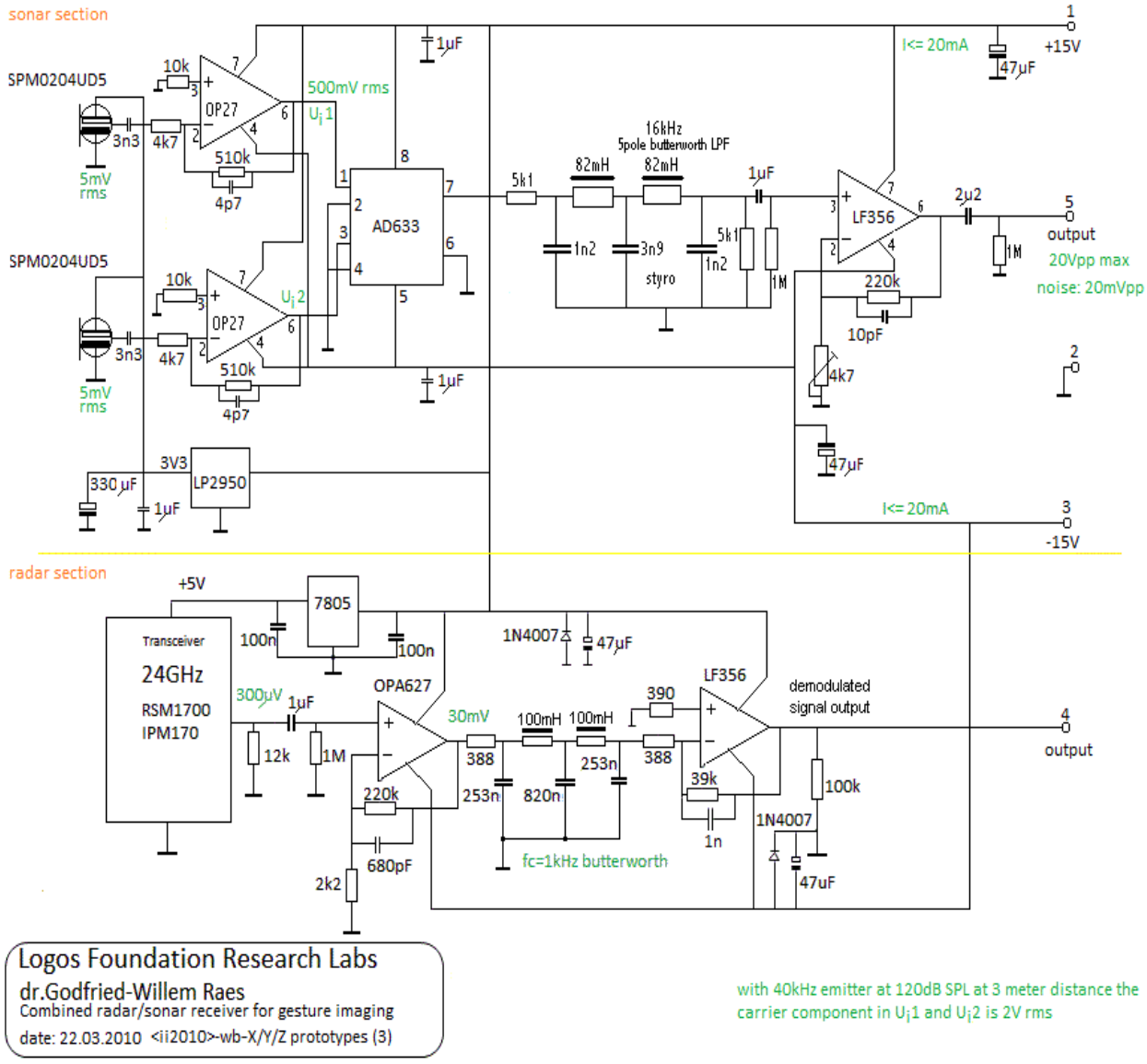

Logos Foundation Research Labs
dr.Godfried-Willem Raes
Combined radar/sonar receiver for gesture imaging
date: 22.03.2010 <ii2010>-wb-X/Y/Z prototypes (3)

with 40kHz emitter at 120dB SPL at 3 meter distance the carrier component in U_i1 and U_i2 is 2V rms

The principle behind the distance measurement technique made possible by this circuit is shown in the graph below, showing the signals for a single small gesture:

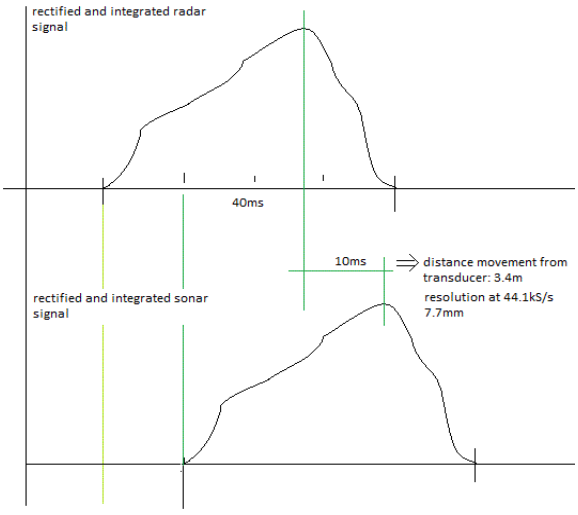

It is generally not possible to find the start of the gesture signal reliably, and hence it is better to

look for a local maximum in the data. Of course latency is introduced this way. Correlation of the two waveforms is a better alternative, in the sense that it gives more reliable distance data, but it is mathematically more intensive and may lead to even more latency. For non real-time applications this is obviously not an issue.

This circuit was built in 3 copies to serve as X, Y and Z receivers. The breadboarded circuits for the upper part (sonar) came out looking like this:

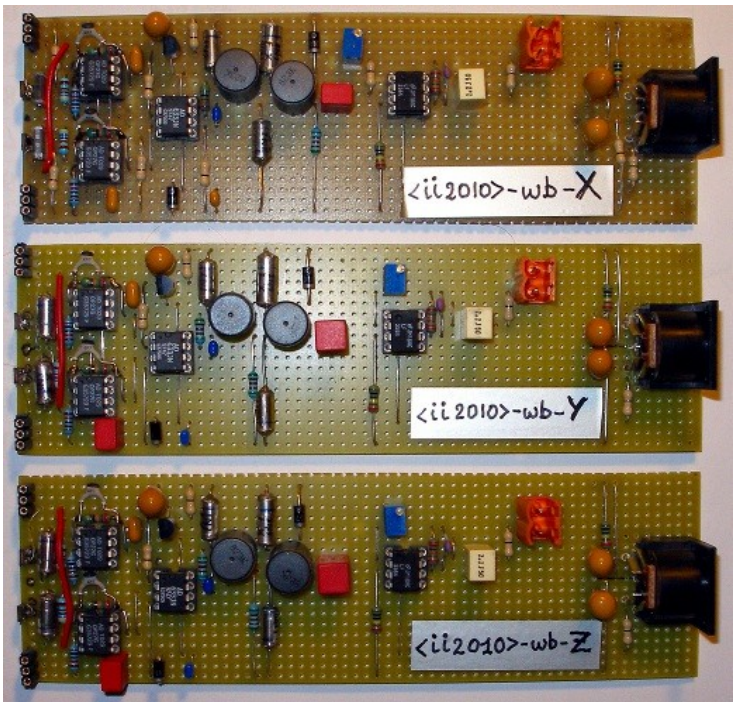

The signal noise ratio measured with this circuit – properly enclosed – attained 60dB. Further improvements are still conceivable and possible: by using B&K ultrasonic measurement microphones in combination with the best available multipliers on the market and by ruling out all offset errors, an improvement of approx. 12dB can be anticipated. The price, however, would also rise by some 40dB... The S/N ratio obtained with the radar section is at least 20dB poorer than that of the sonar section. Hence data analysis should be based on the sonar signal leaving the radar signal for redundancy checks and distance determination only. Spectrum measurements with this system, operated with a 40kHz carrier, revealed that for normal human gestures, no gesture-related frequency components higher than 4kHz are traceable in the sonar signal. A low pass filter with a cut off at 4kHz would have been enough, but can be implemented in software quite easily if the sampling rate is high enough. (11)

In order to test this hardware gesture recognition platform with both sonar and radar sensors, we have made a board to make interfacing to a computer based audio input device (6 channels of audio line level input are required for a complete 3-D gesture rendering) an easy matter. The circuit looks like this:

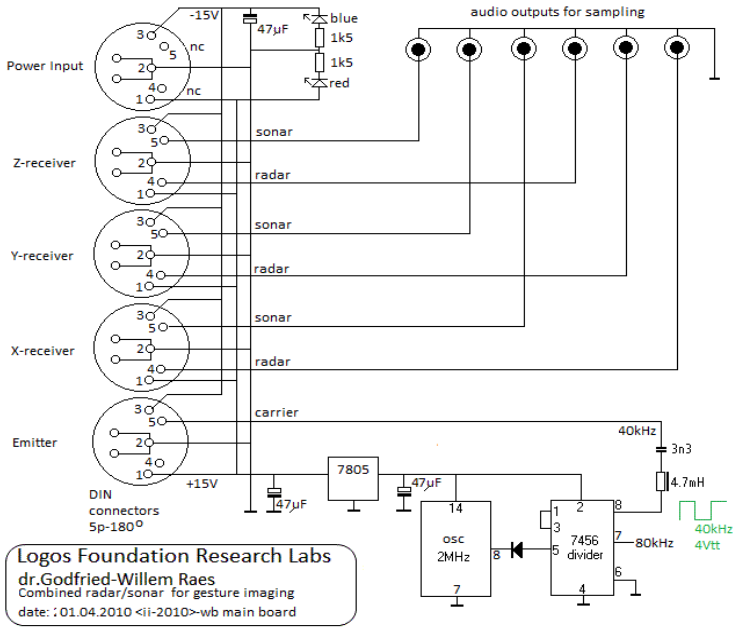

The 7456 divider chip used here is an obsolete TTL part produced by Texas Instruments, no longer in production. Since we had still a good quantity in stock, we used it nevertheless. Software for gesture control of the robot orchestra using this hardware platform has been developed by Kristof Lauwers at the Logos Foundation using PD. Sample code is available on request.

The test board looks like this:

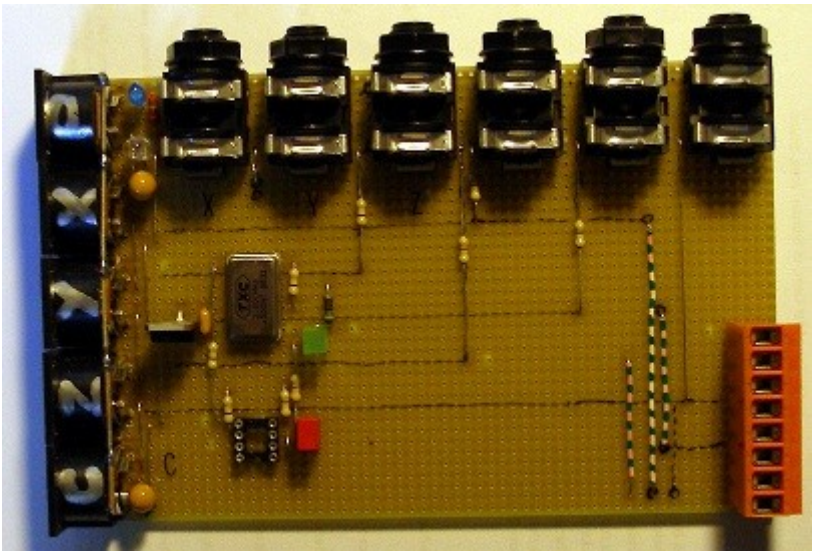

Emitter board:

This small board receives the carrier signal -either fixed frequency or an FM modulated signal- from the analogue computer board described above. The design goal was to achieve a sound pressure level of approx. 120 dB (measured at 1 m distance) with wide area coverage. (7) Basically the circuit is a bridge amplifier delivering an output voltage swing almost twice as large as the power supply voltage. The LF356 was selected for its excellent behaviour in driving capacitive loads.

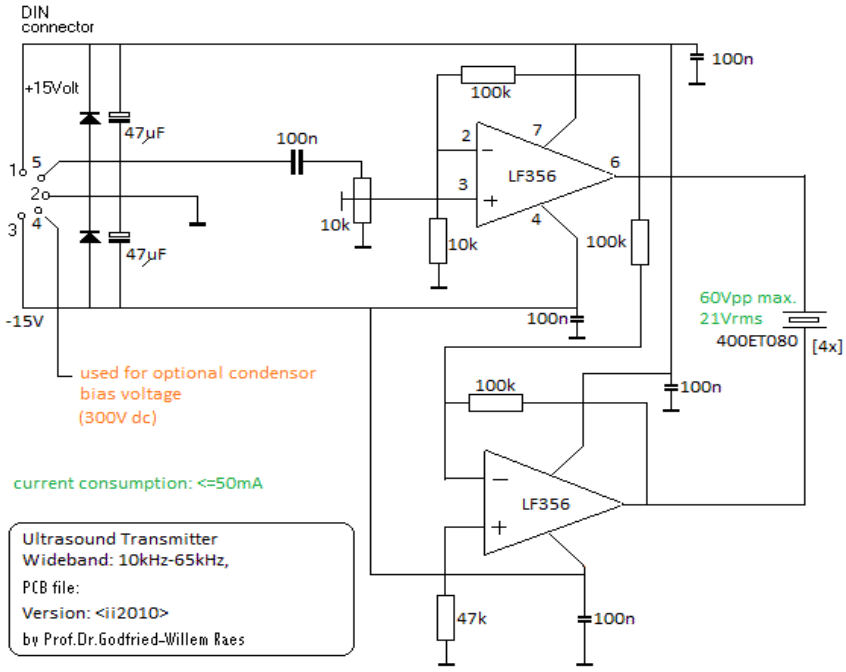

The practical realization looks like this:

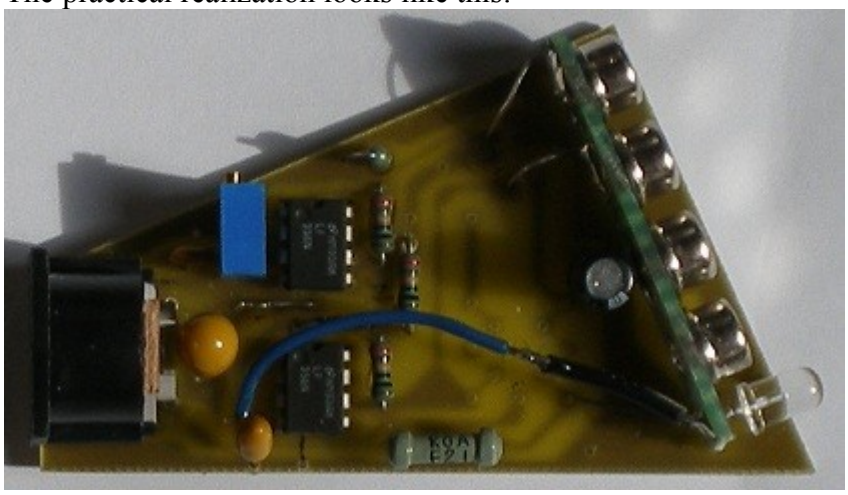

The input potentiometer can be used to adjust the output level such that an optimum S/N ratio is achieved. It also allows adjustment to variable distances in the set-up. In fact, the placement of the emitter does not have to be strictly on the vertex of the ground plane of the imaginary tetrahedron, but can be placed much farther away. The distance to the X,Y and Z receivers however has to be the same. Although not drawn in the circuit drawing, our practical realization of the circuit uses an array of four 400ET080 transmitters, connected in parallel and aligned vertically. The beam angle for these transducers is specified as 125 degrees. The vertical stack alignment was done in an attempt to meet the sound pressure levels that we obtained in using the Murata piezoelectric transducers in earlier designs. These 16mm Murata piezoelectric transducers, however, are quite unidirectional and do not allow frequency modulation due to their inherent sharp resonance at 40 kHz. Sound pressure measurement with this circuit and the 400ET080 transducers revealed that we could not obtain the required 120 dB. Hence we also made a similar circuit, this time using two 10 mm diameter 400ST100 ceramic transducers mounted in a horizontal plane. The modulation bandwidth with these transducers is limited to 2.5 kHz, but 120 dB sound level pressure could be reached. However the voltage over these transducers should be kept below 15 V_{rms}. The capacitance of the transducers is 1900 pF and the beam angle limited to 72 degrees.

The required sound pressure level could be reached with the circuit below. Here we used an array of

four Murata MA40S4S emitters, specified for 120dB SPL at 30cm. The beam angle for each transducer is specified as 80 degrees, thus in order to have a somewhat wider coverage, we arranged the array of four transducers in a square on an imaginary sphere segment. Each transducer has a capacitance of 2.55nF and hence the total capacitance (10.2nF), if we connect them all in parallel, would marginally exceed the capacitive drive specification for the LF356 opamps. We tried this, and in fact observed a very odd phenomenon in that the lower opamp undergoes a complete phase reversal as soon as the input signal exceeds a certain limit, yielding almost no output from the circuit. Hence we used the series/parallel connection as shown in the circuit below. Since we had plenty of headroom – the transducers should not be driven with voltages higher than 20Vpp – we suffered no penalty from this.

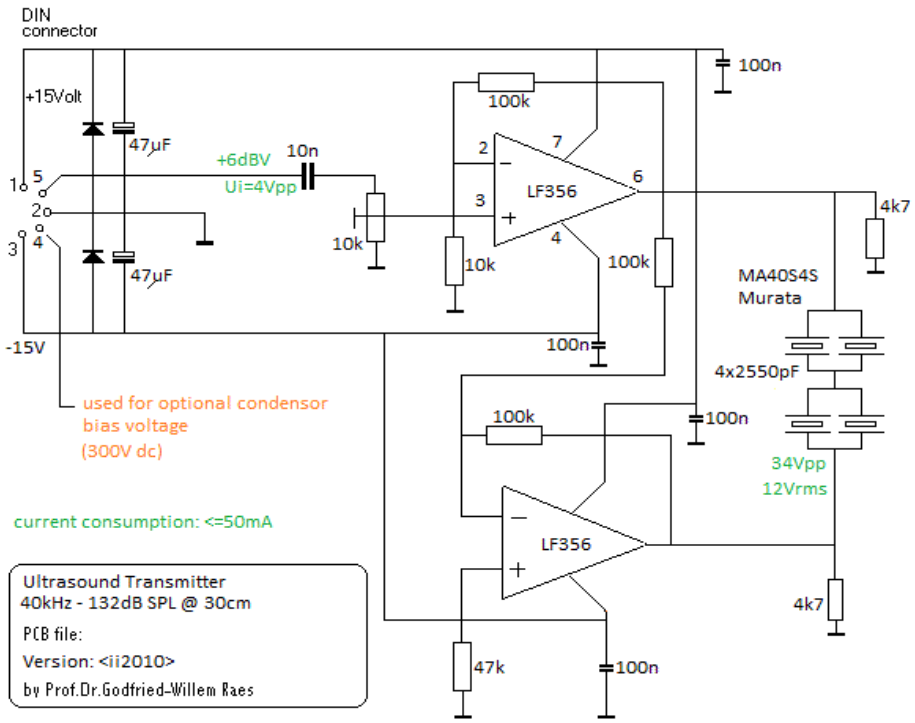

Although we now meet the sound pressure level requirements, this circuit does not lend itself very well to FM-modulation due to the small bandwidth of the transducers.

Other experiments carried out have been:

1.- Extended range tweeter loudspeakers: highly inefficient, very bulky and... way too directional. Imagine: we needed a 150 W amplifier to feed a 200 W titanium dome tweeter in order to get 120 dB sound pressure at 40 kHz at 1 meter distance.

2.- Capacitive transducers requiring a DC bias voltage in the order of 300 V. Their principle of operation is identical to that of electrostatic loudspeakers. These work pretty well and they are indeed suitable for FM applications, but due to their large diaphragms, they are also way too directional (12 degrees) for our application here. The type we tested is 500ES430, although specified for 50 kHz, they also operate well at 40 kHz. A particular problem is raised by the required +300 V bias: if this voltage is applied through the 5 conductor cable, the latter becomes highly microphonic itself. Generating this voltage with a small switcher on board, on the other hand, causes a lot of interference with the ultrasound carrier. A more clever circuit, in which the DC voltage is obtained through diode multiplication starting from the carrier signal itself, should be designed.

3.- Plasma ion sources are a perfect match on the design table: They are by nature omnidirectional and can easily cope with FM. However, they are highly sensitive to air flow – they sputter – and

they cause extreme EMC in the environment. The fact that they are intrinsically dangerous as they operate with 20 kV voltage levels, also limits their usability. (6)

The ideal transmitter has not been found so far. The importance of the search for very powerful transmitters lies in the simple fact that the signal to noise ratio at the receivers end, tracks perfectly with the sound pressure level of the transmitters. Research goes on.

A final note on interference.

In general, sonar technology is far less sensitive to environmental interference, although care must be taken to avoid turbulences and wind flow as well as temperature gradients. However, another source of interference is formed by the extended spectral contents of quite a few sounds of real musical instruments. This interference does not occur with loudspeaker-generated environmental music, since audio systems filter out all frequency components above 20 kHz by their very nature. Since we use this technology in the implementations of our invisible instrument to control our robot orchestra, composed of purely acoustical sound sources, we have often noticed disturbances with certain loud sounds such as those that originate from our robot saxophone <Autosax>, struck metal shells in <Llor> and edge whistle tones generated by organ pipes in our <Qt>, <Bourdonola> and <Piperola> robot. The problem can be avoided only by placing the sensor system far enough from the acoustical sound sources. Unfortunately, on our premises at the Logos Foundation this is impossible because of lack of space...

Dr. Godfried-Willem Raes

Notes:

(1) This project is part of the ongoing research of the author into gesture-controlled devices over the last 35 years. Earlier systems, based on sonar, radar, infra-red pyro-detection and other technologies are fully described in "Gesture controlled virtual musical instrument" (1999) as well as in his doctoral dissertation 'An Invisible Instrument' (1993). Artistic productions and compositions using these interfaces and devices have been: <Standing Waves>, <Holosound>, <A Book of Moves>, <Virtual Jews Harp>, <Songbook>, <Slow Sham Rising>, <Gestrobo>, <Quadrada>, <Technofaustus> , <Butoh>, <Ices>, <Bodies of revolution>, <Differentials> etc.

(2) As of August 16th 2009 the world record for running in the 100m sprint is fixed at 9.58 s. This corresponds to a movement speed of 10.52 m/s or 37.8 km/h. Needless to say that such speeds are not encountered amongst 'normal' people, not even when they get involved in the wildest forms of dancing.

$$f_d = 2 \, v \, f_o \cos(a) / c$$

- f_o = frequency of the carrier (ca. 40 kHz)
- c = propagation speed of the wave (340 m/s)
- f_d = Doppler frequency
- v = movement speed of the body
- a = movement angle with the axis of the transducer

(3) Here is the circuit as we developed it for the Monacor electret MCE2500 microphone:

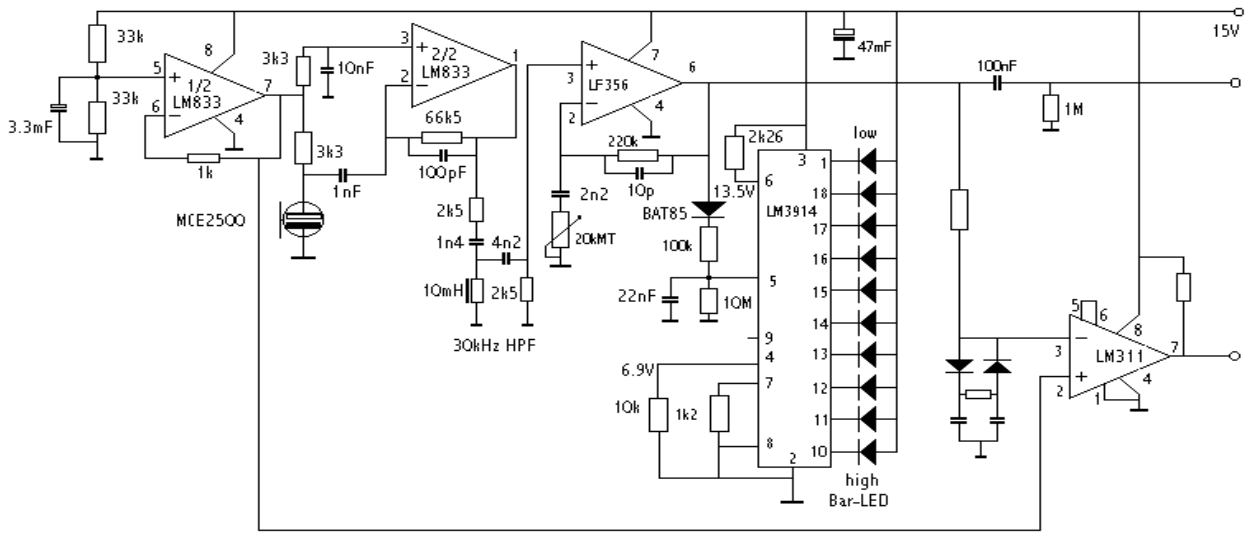

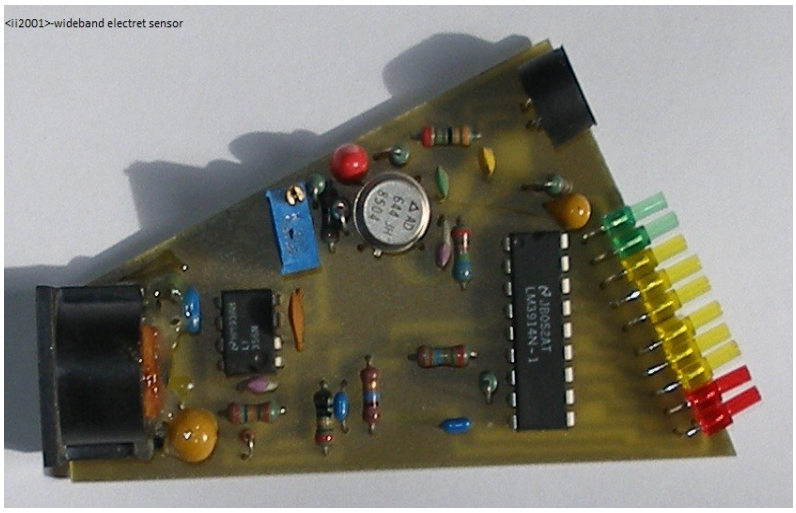

This circuit has very good wide band characteristics but suffers from a poorer signal noise ratio.

(4) Here is the circuit as we developed and tested it with the Prowave 400FS060 sensor:

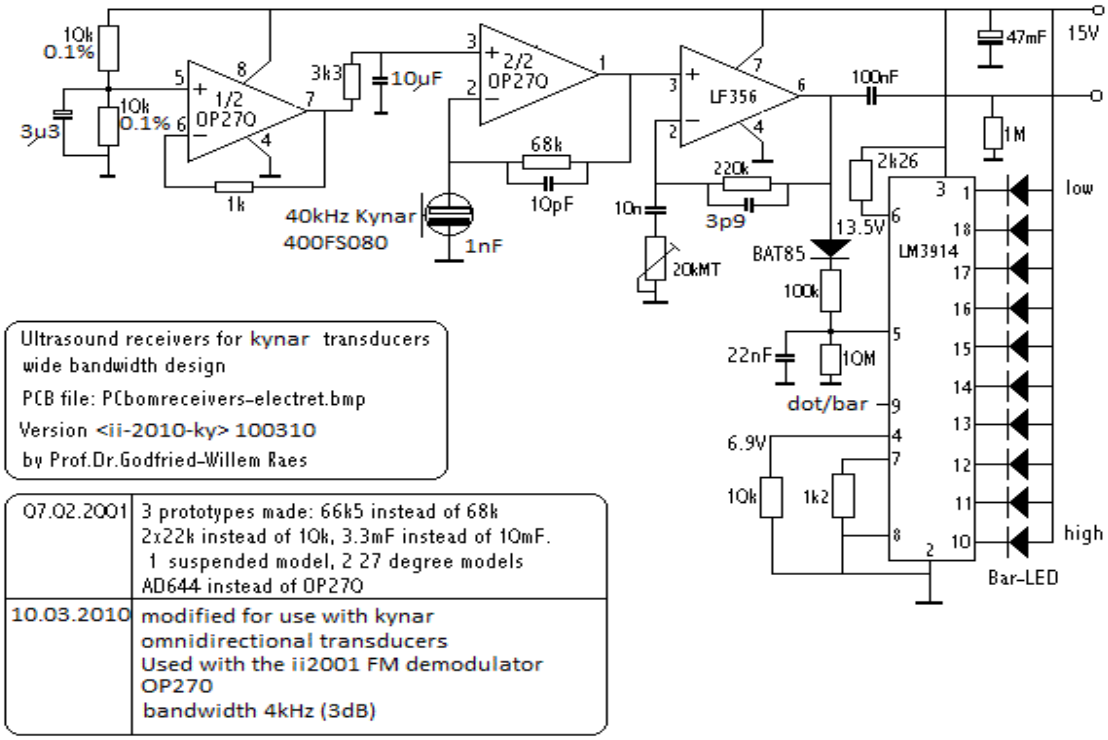

(5) for a more in-depth treatment of FM modulation for distance determination see: RAES, Godfried-Willem "Microwave Gesture Sensing" (Ghent, 2009)

(6) See our design for a real digital loudspeaker: Talking Flames. Since the sound source here is a virtual point, the radiation pattern is inherently spherical.

(7) Most data sheets for ultrasound transmitters specify the SPL measured at a distance of only 30 cm, whereas the standard for acoustic measurements specifies it at a distance of 1 m. This means that we have to subtract approx. 12 dB to bring the data back to common standards. Also note that in our set-up, the distance between emitter and receiver is normally 3 m. This means that the SPL at the point of the receiver will be 20 dB down compared to the SPL as given in the data sheets.

(8) Transducer data comparison table:

Brand	Type	technology	frequency fc	sensitivity (receiving)	SPL (output)	beam angle	bandwidth	S/N
Murata	MA40S4R	piezo	40kHz	-63dB	-	80		
Murata	MA40S4S	piezo	40kHz	-	120dB(@30cm)	80		
ProWave	400FS080	PVDF film	40kHz		95dB (@10cm)	360/80	4kHz	
ProWave	800FS049	PVDF film	77kHz			360/80		
Knowles	SPM0204UD5	MEMS	10-65kHz	-47dB	-	omni (360)	55kHz	-59dB
ProWave	400ET080	piezo (closed)	40kHz	-	100dB(@30cm)	125	1.5kHz	
ProWave	400ER080	piezo (closed)	40kHz	-80dB		125	2 kHz	
ProWave	400ST10(0)	piezo	40kHz	-	112dB(@30cm)	72	2.5kHz	
ProWave	400SR10(0)	piezo	40kHz	-70dB		72	3kHz	
ProWave	400ST16(0)	piezo	40kHz	-	120dB(@30cm)	55	2 kHz	
ProWave	400SR16(0)	piezo	40kHz	-65dB		55	2.5 kHz	
ProWave	500ES430	electrostatic	50kHz	-42dB	119dB(@50cm)	12.8		
Monacor	MCE2500	electret	20Hz-65kHz	-46dB	-	cardiod	65kHz	-58dB

(9) The radar system for gesture measurement is described in more detail in Raes, Godfried-Willem, "Microwave Gesture Sensing"(Ghent, 2009)

(10) The software used for making sense of all the signals described here is treated in the second part of this paper:

"Namuda Gesture Recognition"(Ghent, 2010)

(11) The system described here was used for an exhaustive measurement session lead by Dr. Jin Hyun Kim during the second week of May 2010. The sonar receiver signals were recorded as audio tracks simultaneously with the audio of the M&M robot orchestra playing under the control of our own Namuda gesture recognition software referred to in the previous note. At the same time, a high speed video recording (300fps) of all gesture input was made, thus providing a very wide data set for further analysis and research. A paper presenting the results of this investigation will be published in due time.

(12) A word of warning with regard to the measurement of the signal voltage levels may be appropriate here: if using a multimeter with a true RMS scale, check the characteristics of the meter beforehand. The large majority of such instruments cannot handle AC signals with frequencies up to and above 40 kHz. Even good and expensive ones, such as the Agilent U1252A, is only reliable up to 30 kHz. The Fluke 87 performs well in this respect. The instrument of choice for voltage measurement therefore remains the oscilloscope, though is is a bit clumsy to take on the road...

Bibliographical references:

- Analog Devices, AD633 data sheet and application notes, 2002.
- BECKMANN, Petr & SPIZZICHINO, Andre "The Scattering of Electromagnetic Waves from Rough Surfaces", Pergamon Press, Oxford, 1963
- DROITCOUR, Amy Diane "Non contact measurement of hearth and respiration rates with a single-chip microwave Doppler radar", Stanford PhD thesis, June 2006.
- RAES, Godfried-Willem "Een onzichtbaar muziekinstrument" (Gent, 1993, Ph.D. thesis)
- RAES, Godfried-Willem "An Invisible Instrument (1994)
- RAES, Godfried-Willem "Gesture controlled virtual musical instrument" (Ghent, 1999)
- RAES, Godfried-Willem "Quadrada" (Ghent, 2003)
- RAES, Godfried-Willem "PicRadar" (Ghent, 2004-2005)
- RAES, Godfried-Willem "Distance sensing devices" (Ghent, 2007)
- RAES, Godfried-Willem "Microwave Gesture Sensing"(Ghent, 2009)
- RAES, Godfried-Willem "Namuda Gesture Recognition"(Ghent, 2010)
- SAMRASH Company "Users Manual for the Bumblebee", (05.2008) http://www.samraksh.com/support.html
- Microwave Solutions Ltd. 'MDU11xx series tunable transceivers', 2008
- MENDE, Ralph, BEHRENS, Marc "A 24GHz ACC Radar Sensor", 02/2005, Smart microwave sensors Gmbh
- SINCLAIR, Ian Robertson., "Sensors and Transducers" (London, 1992) , ISBN 0 7506 0415 8

Last update for this chapter:2010-05-26

2

<Namuda Gesture Recognition on the Holosound ii2010 platform>

by

Dr. Godfried-Willem Raes

post-doctoral researcher
Ghent University College & Logos Foundation

2010

This paper describes the software layer for gesture recognition using Doppler-based hardware systems. For a good understanding, it is advised that readers familiarize themselves first with the hardware described in "Holosound 2010, a Doppler sonar-based 3-D gesture measurement system". This paper is part of a triptych in which the final part will delve further into the expressive meaning of gesture and artistic aspects of the namuda dance project developed at the Logos Foundation.

The holosound hardware is connected to the PC for sampling and further analysis, treated in this preliminary draft of a paper. It is very important to stress that all the data acquisition and classification procedures covered here were designed to work concurrently and in real time. The latency was to be better than 10ms. This restriction accounts for the fact that we did not optimize the procedures for maximisation of precision nor for maximisation of feature extraction. It will be obvious that taking this restriction away, and performing the analysis off-line, can greatly improve the functionality of the gesture sensing technology for analytical and scientific purposes.

1. Data Acquisition:
Since the low pass filtering is performed in the hardware, we can set up a three-channel sampler with a sampling rate of 1024 S/s. Using a National Instruments USB data acquisition device (type: NI-USB 6210 or NI-USB 6212) and calling in the drivers and libraries offered by NiDAQmx, this is pretty easy. The resolution is 16 bits and the voltage sensitivity for the inputs is programmed for -10 V to +10 V. There is plenty of headroom, so we should not fear clipping, since the signals from

our hardware stay well within the range of 4 V_{pp} under normal circumstances. The data is read in a callback function operating at a rate of 256 times a second. So on each call, 3 x 4 = 12 new samples are read. Reading the data at the sampling rate itself is impossible due to limitations in the USB driver implementation provided by National Instruments, despite the fact that the devices themselves can handle sampling rates well above 250 kS/s.
These samples are written to the fast circular data buffers, 256 entries in size, one for each of the three vectors. Thus the time window available here is 250 ms and the sampling rate remains at 1024S/s.
A medium size time window is set up in the same callback for which we down-sample to 256 S/s and write the result to the medium data buffers. Thus these circular buffers cover a time window of 1 second, or, 256 samples. The down-sampling applies a simple low pass filter to the data.
A long time window, covering a 4-second timespan, is then implemented by down-sampling again to 64 S/s. These circular buffers again contain 256 samples.
Pointers to these nine circular buffers are made available to the user through a specific structure. All buffer data is in double precision format and normalized, bipolar -1 to +1.

Further preprocessing performed from within the same callback consists of:

A. setting up a running integrator with rectification in order to calculate the signal strength proportional to the size of the moving and reflecting body. These values are returned in the normalized .xa(), .ya(), .za() fields of the structure. The integration depth can be controller with the parameter in the .dta field.
The algorithm here also implements a high pass filter to eliminate slow DC offsets and artefacts originating from very slow and mostly involuntary movements of the body.
To summarise, body surface derivation uses:

```
high pass filter
rectifier
low pass filter
integrator
```

B. Calculation of the frequencies in the Doppler signals in order to grasp information on the speed of movement. Here we encounter quite a few fundamental problems: first of all, the signals are in no way periodic but in fact bandwidth limited noise bands. Second, the frequency limits of these Doppler signals depend on the angle of the movement: the cosine in the Doppler formula $f_d = 2 \text{ v } f_o \cos(a) / c$. Only when movements are performed towards or away from a particular vector in line with the transducer, will the cosine be unity and the absolute value of the bandwidth trustworthy. If the performer knows this, he/she can obviously take it into account. For general gesture analysis though, ideally the coordinates of the movement in space have to be known. As we have proved in our papers and notes on hardware for gesture recognition, this can be solved either by combining sonar and radar systems, or by FM modulating the carrier wave. This adds a lot of complexity to the software and we will not delve deeper into the related problems at this point.
However, even without cosine correction and lack of positional information, we can reduce induced errors greatly by making use of the redundancy offered by the fact that we have three vectors of data available. Placing the sensors on the vertices of an imaginary tetrahedron means that the maximum value for detected speed in the three vectors together can never be more than 50% off, the cosine of 60 degrees being equal to 0.5.
The algorithm performed in the callback function first converts the data in the fast buffer to a square wave with a Schmitt trigger and hysteresis to avoid noise interference. Then the zero crosses of the signal are counted, disregarding any periodicity. Thus the results, returned in the .xf(), .yf(), .zf() fields of our structure, reflect noise densities of the signal proportional to movement speed. The numeric values returned are not normalized but reflect real world values expressed in Hz, but have

to be interpreted carefully within the constraints as explained. If normalization is required, the values can be simply divided by 200, a realistic maximum value as determined empirically.

C. Calculation of vectorial acceleration. This is done by differentiating the vectorial frequency information. The delta-t value can be user controlled via the .dtacc parameter. Larger values lead to better resolution, to the detriment of responsiveness. The results are returned in .xac(), .yac(), .zac(), with the scaling being independent from the setting for .dtacc.

This callback function updates the parameter fields in the Doppler structure 256 times a second. This is the first level of processing of the movement data. It yields information on the moving body surface as well as a first approximation of speed.
Performing FFTs on the data buffers from within the same callback is impossible, even on a quad core PC. Therefore the spectral analysis of the data must be performed as a different thread. The shape of the spectrum (the distribution of the frequency bands) reflects the characteristics of the gestures very well. This can be demonstrated convincingly by mapping the output of the transform on the keys of a piano, whereby the power of each frequency band is mapped on the velocity of the attack for each key.

The complete structure as declared in the software is:

```
TYPE DopplerType DWORD      ' for ii_20xx with NiDAQmx
     xa     AS SINGLE       ' reflection amplitudes for the x-vector
     ya     AS SINGLE       ' idem for y-vector
     za     AS SINGLE       ' idem for z-vector
     xf     AS SINGLE       ' doppler frequency shift density for the x-vector
     yf     AS SINGLE
     zf     AS SINGLE
     xac    AS SINGLE       ' acceleration for the x-vector
     yac    AS SINGLE
     zac    AS SINGLE
     pxfast AS DOUBLE PTR   ' pointer to the x-vector data(0). Most recent data are in data(255) 250 ms buffer  1024 S/s
     pyfast AS DOUBLE PTR
     pzfast AS DOUBLE PTR
     pxm    AS DOUBLE PTR   ' 1s buffer, sampling rate 256 S/s
     pym    AS DOUBLE PTR
     pzm    AS DOUBLE PTR
     pxslow AS DOUBLE PTR   ' 4s buffer, sampling rate 64 S/s
     pyslow AS DOUBLE PTR
     pzslow AS DOUBLE PTR
     pxfbuf AS SINGLE PTR   ' 64 values for the frequency measurement, used for calculation of acceleration
     pyfbuf AS SINGLE PTR   ' sampling rate: 256 S/s
     pzfbuf AS SINGLE PTR   ' most recent data in data(63)
     dtacc  AS WORD         ' dt for acceleration derivation. Valid values: 1-63. Do not exceed range!
     dta    AS WORD         ' amplitude integration depth  (0-255)
     noise  AS SINGLE       ' noise level threshold   (1E-3, default, for 60 dB signal noise ratio)
     hpf    AS WORD         ' high pass filter differentiation depth
END TYPE
```

2. Gesture recognition

Although the callback function described above already performs quite a lot of data processing and allows us to get elementary information on the movement of the body, it is not capable of performing gesture recognition. Hence the next steps. In our approach, rather than trying to recognize predefined gesture models, we attempt to maximize the number of gestural characteristics retrievable from the use of this particular hardware and its signals as used throughout thousands of experiments with more than 20 different human bodies. The subjects were either trained musicians or dancers operating with direct auditory feedback. We baptised these retrievable gestural characteristics as Namuda gesture prototypes. Each prototype is defined within a certain time frame (100 to 1000 ms) and has a calculated normalized property strength as well as a persistence value, expressed in time units (generally 1/256 second units, corresponding to the best possible resolution within the constraints of our sampling function).

Namuda gesture types: (3)

So far we are able to distinguish twelve types of gesture (not counting the no-movement property, 'Freeze'). We certainly do not exclude the possibility of deriving a few more, but on the other hand we have found that these twelve micro-gestures might very well be already at the upper limit of what we can clearly control given the motor skills of our bodies. Many gestural characteristics can be seen as dipoles: they exclude each other. Dipoles we distinguish are:

1.- Speeding up versus slowing down

speedup
definition: the movement speed goes up within a time frame of maximum 500 ms

slowdown
definition: the movement speed goes down within a time frame of maximum 500 ms

2.- Grow - Shrink (or, expansion - implosion)

exploding
definition: the size of the moving body surface increases within a time frame of maximum 1000 ms

imploding
definition: the size of the moving body surface decreases within a time frame of maximum 1000 ms

Algorithms for feature extraction:

Speedup/slowdown and implode/explode use a gesture recognition algorithm based on a FIR filter. The coefficients used are the elementary gesture type that we are trying to evaluate. In the first approach these coefficients are linear functions. Further refinement consists of applying different functions to calculate the coefficients: quart sine or cosine, exponentials or even beta functions. However, this should only be done on the condition that the pattern recognition triggers the property with linear coefficients. The reason being that we simply do not have enough computing power to handle each recognition algorithm with many different coefficient models in real time.
The procedure is implemented as a function to which the pointer to the frequency data array (covering 500 ms) is passed as well as the vector. Vectors are numbered 0,1,2 for the x, y, and z vertexes where the transducers are placed physically. Vector 3 always refers to a sum or a maximum value. (2)

```
SUB GestureProp_Speedup (BYREF ar() AS SINGLE, BYVAL vektor AS LONG)
    'time weighted moving average approach using a Nth order FIR filter
    'vector: 0,1,2  for x,y,z
    'speed data   - the coefficients are the shape of a speedup gesture (rising)

    LOCAL i AS DWORD
    LOCAL av AS SINGLE
    STATIC order AS LONG
    STATIC Fscale  AS SINGLE
    DIM oldF(0 TO 2) AS STATIC SINGLE

    ' speedup coefficients, these have only to be recalculated if the window size is changed with .Forder:
    IF order <> gesture.Forder THEN
        order = gesture.Forder
        REDIM bs(0 TO order) AS STATIC SINGLE
        RESET Fscale
        FOR i = 0 TO order
            bs(i) = i / order                'rising series of coefficients: this is the gesture model
        NEXT i
        Fscale = (order + 1) / 2             'for normalization
```

```
    END IF

    'FIR with time dependent linear coefficients:
    FOR i = (UBOUND(ar) - order) TO UBOUND(ar)
            av = av + (ar(i) * bs(i-UBOUND(ar) + order))
    NEXT i

    'now we calculate the matching value (fuzzy):
    IF av > oldF(vektor) THEN
          gesture.speedup(vektor) = (av - oldF(vektor)) * 2
          INCR gesture.speedup_dur(vektor)
    ELSE
          RESET gesture.speedup(vektor), gesture.speedup_dur(vektor)
    END IF
    gesture.speedup_val(vektor) = av/ Fscale 'this is the renormalised output value of the filter itself
    oldF(vektor) = av

    'reconsider the global property (vektor 3):
    Gesture.speedup(3) =  MAX(Gesture.speedup(0), Gesture.speedup(1),Gesture.speedup(2))
    Gesture.speedup_val(3) =  MAX(Gesture.speedup_val(0), Gesture.speedup_val(1),Gesture.speedup_val(2))

END SUB
```

Here is a plot of the result of this algorithm:

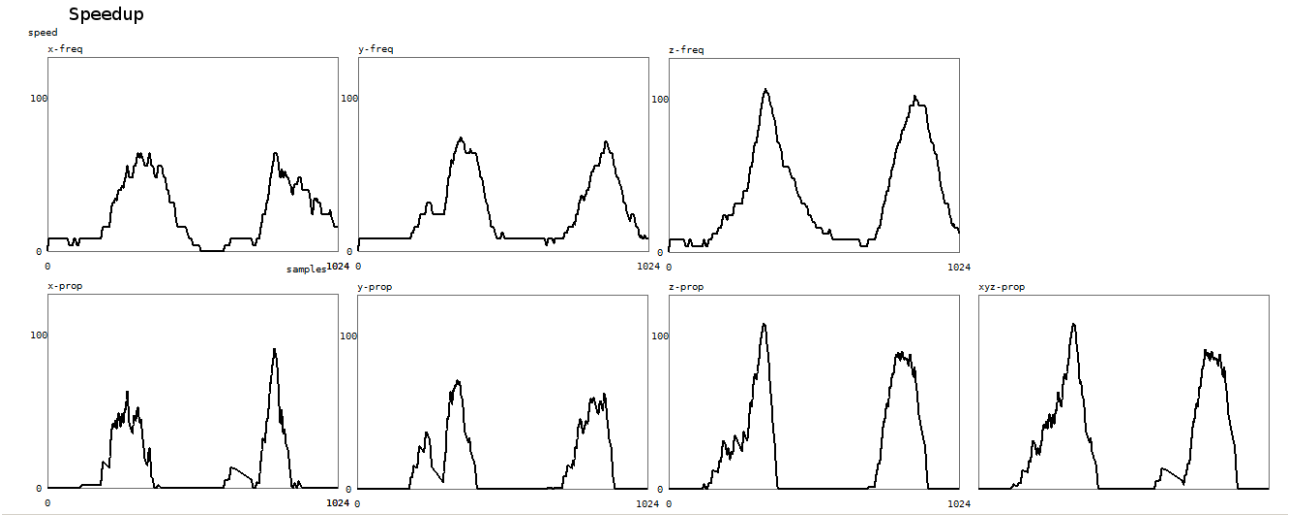

The upper three graphs give the frequency signals for the x,y and z vectors as found in pDoppler.xf, yf, zf. Vertical scale is in Hz. The window shows a time frame of 4 seconds. The graphs below show the output of the recognition. The vertical scale shows property strength, again for the three vectors. The last graph shows the property for all three vectors together.
The procedure for slowdown recognition is identical, but the coefficients are a linearly descending series.

Here is a plot of the result of the slowdown recognition algorithm:

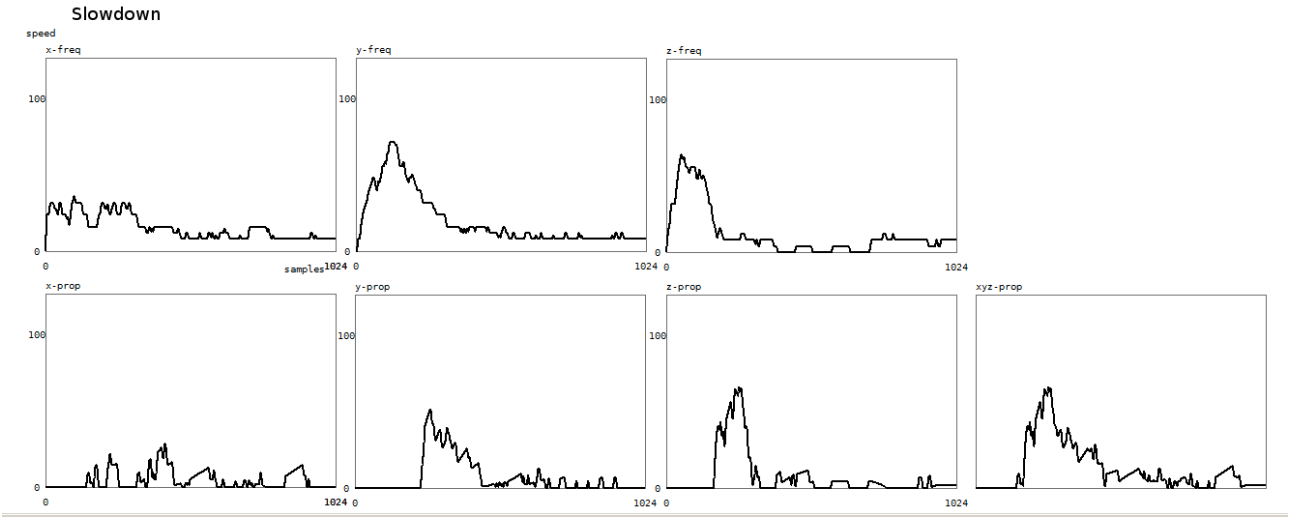

For shrinking/expanding body surface we use the same approach but found that the time window has to be made larger for good reliability. We have it set at 1 second. The FIR filter order can be changed by the user using the parameter in the .Sorder field.

Here is the procedure for shrinking gesture recognition with linear coefficients:

```
SUB Gestureprop_Shrink ((BYREF ar() AS SINGLE, BYVAL vektor AS LONG)
    ' pattern recognition code using FIR approach with the gesture model based in the coefficients
    ' since this works with our omnidirectional ii2010 receivers , no angle correction is required
    ' the amplitudes of the reflected signals are independent from the frequency of the doppler shift.

    LOCAL i,j AS DWORD
    LOCAL av, s AS SINGLE
    STATIC order AS LONG
    STATIC Sscale  AS SINGLE
    DIM oldS(2) AS STATIC SINGLE
    DIM bs(gesture.Sorder) AS STATIC SINGLE

    'calculation of a descending series of coefficients:
    IF order <> gesture.Sorder THEN
        order = gesture.Sorder
        REDIM bs(order) AS STATIC SINGLE
        RESET Sscale
        FOR i = 0 TO order
            bs(i) = 1 - (i/(order+1))       'this could also be the result of a beta-function describing the gesture type
            Sscale += bs(i)                 'sum of factors, required for normalisation.
        NEXT i
    END IF

    'FIR filter with time dependent linearly descending coefficients:
    RESET j
    FOR i = (UBOUND(ar) - order + 1) TO UBOUND(ar)
            av += (ar(i) * bs(j))
            INCR j
    NEXT i

    'now classify: shrinking surface
     IF (av < oldS(vektor)- (@pDoppler.noise/ SQR(order)))  AND (av/Sscale > @pDoppler.noise) THEN
          IF gesture.implo_dur(vektor) THEN
                   gesture.implo(vektor) = MAX(MIN((oldS(vektor) - Av)* 2.5, 1),0)
                                                'scaling factor for commensurability with the explo property
                                                'observed range, before rescaling with * 2.5:
                                                '19.04: x<= 0.156, y<=0.224, z<=0.08  [gwr with clothes]
                                                '19.04: X<= 0.335, y<=0.373, z<=0.268 [gwr naked]
          ELSE
                  RESET gesture.implo(vektor)
                                                'the property will only be set if it lasts at least 7.8ms
          END IF
          INCR gesture.implo_dur(vektor)        'in 1/256s units (3.9ms).
     ELSE
                  RESET gesture.implo(vektor), gesture.implo_dur(vektor)
     END IF
     gesture.implo_val(vektor) = av/ Sscale   'we always return this normalized value for research purposes.
     oldS(vektor) = av

    gesture.implo(3) =  (gesture.implo(0) * gesture.implo(1) * gesture.implo(2)) ^0.33   'to be further investigated
    gesture.implo_val(3) =  (gesture.implo_val(0) * gesture.implo_val(1) * gesture.implo_val(2)) ^0.33


END SUB
```

Here is a plot of the result of the implosion algorithm:

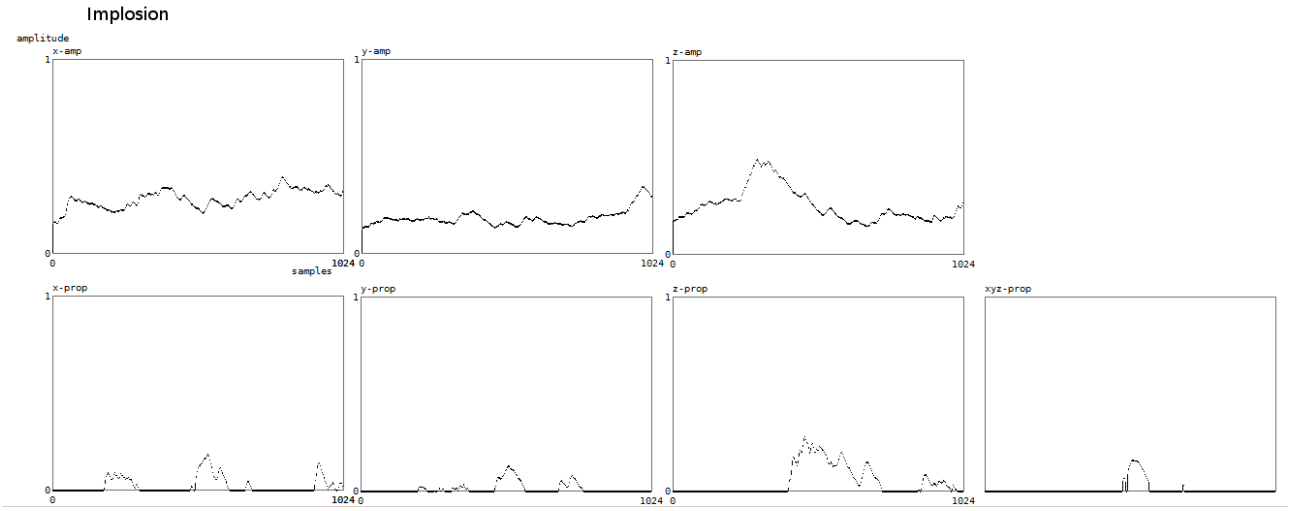

In this case we plot the normalized amplitudes of the Doppler signals against time (4 seconds) in the upper three graphs. Below, again, is property strength.

For explosion we get similarly:

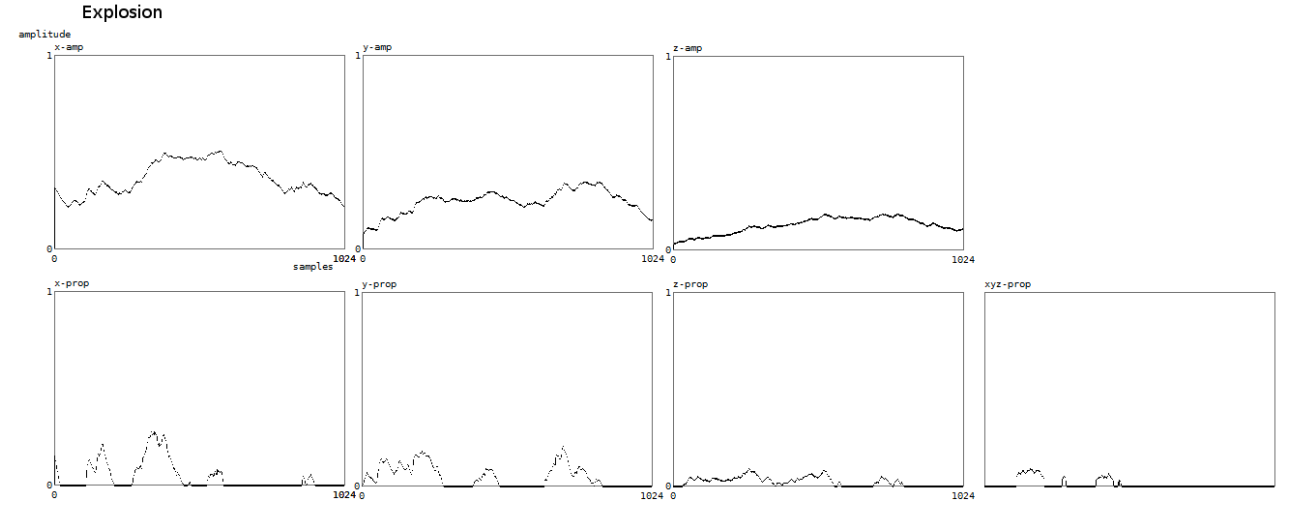

3. Fluency and speed properties

Not all gesture properties are calculated with this or a similar FIR algorithm. For the properties fluency (constancy of moving body surface within the time frame) and fixspeed (constancy of movement speed within the time frame), we found traditional statistics useful. Here we look in the data buffer and calculate the running average as well as the significance. The smaller the deviation from the mean, the stronger the property will be evaluated.
Here is, as an example, our coding for fluency detection:

```
SUB Gestureprop_Fluent ((BYREF ar() AS SINGLE, BYVAL vektor AS LONG)
    LOCAL avg, d, s AS SINGLE
    LOCAL i AS DWORD
    STATIC maxval, maxprop AS SINGLE

         ' calculation of the average in the body surface data array:
        FOR i = 0 TO UBOUND(ar)
            Avg +=  ar(i)
        NEXT i
        Avg /= (UBOUND(ar) +1)        'normalised 0-1

        'calculate the standard deviation:
        FOR i = 0 TO UBOUND(ar)
            d += ((ar(i) - Avg)^ 2)     ' method of the smallest squares
        NEXT i                            ' d =  average fault for each sample
        s = SQR(d/(UBOUND(ar)-1))         ' s = standard deviation for a random population

            ' statistics math memo:
            ' 68% of all values in dta are between Avg - s and Avg + s
            ' 95%                      are between Avg -2s and Avg +2s
            ' 97%                      are between Avg -3s and Avg +3s

            IF Avg > @pDoppler.noise * 5  THEN
                IF gesture.flue_dur(vektor) THEN
                    gesture.flue(vektor) = MAX(0, 1 - (5*s / Avg))     'gives quite a good range
                ELSE
                    RESET gesture.flue(vektor)
                END IF
                INCR gesture.flue_dur(vektor)
            ELSE
                RESET gesture.flue(vektor), gesture.flue_dur(vektor)
            END IF
            gesture.flue_val(vektor) = Avg                          ' always returned.

        Gesture.flue_val(3) = (Gesture.flue_val(0) * Gesture.flue_val(1) * Gesture.flue_val(2)) ^ 0.33  ' questionable
        gesture.flue(3) = (gesture.flue(0) * gesture.flue(1) * gesture.flue(2)) ^ 0.33

END SUB
```

Here is a plot of the result of the fluency property algorithm:

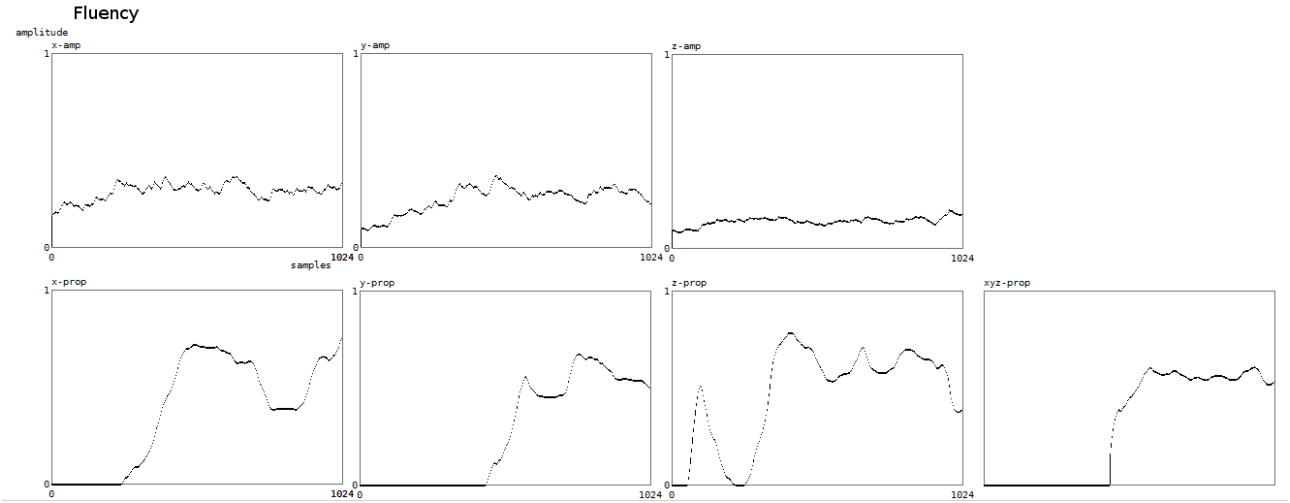

`

And here, again for the speed constancy property:

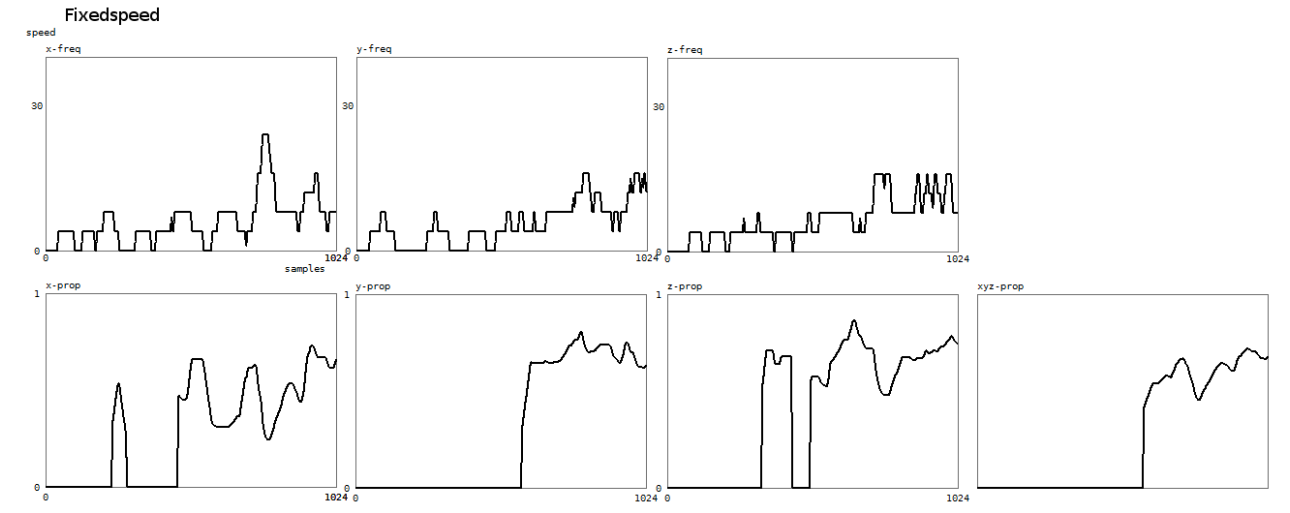

4. Collision - Theatrical Collision

For the dipole collision/theatrical collision, we use yet another approach, based on an analysis of the acceleration data acquired in the sampling callback. The time window used in this analysis is 100 to 390 ms. The smaller values make the algorithm more responsive.
We define the collision property as follows:
the acceleration rises up to the point of collision, where we have a sudden sign reversal.
And, the theatrical collision as:
the acceleration goes down to the point of collision - a standstill - , where we have a small sign reversal followed with a rise of acceleration.

Algorithm:
a first leaky integrator is applied on the first 3/4th's of the acceleration data (upval) and a second integrator on the last quart of the data (downval). The sensitivity is set with the variable sens.
If now upval > sens and downval < - sens, we set the collision property.

The practical coding is as follows:

```
SUB Gestureprop_Collision (BYREF ar() AS SINGLE,  BYVAL vektor AS LONG)
    ' the array passed should be the amplitude array, we need it to look up the impact value on the moment of the collision
    ' we could also pass the value ar(230) alone.
    ' the algo uses a leaky integrator, not FIR!, on the acceleration data
    ' the procedure returns the gesture properties collision and theatrical collision. These are mutually exclusive.
    STATIC tog AS LONG
    STATIC xslope, yslope, zslope, xdown, ydown, zdown, sens AS SINGLE
    IF ISFALSE tog THEN
            sens = 0.4                      ' this is a critical value to experiment with
            DIM xc(25) AS STATIC SINGLE     ' 101 ms buffers for acceleration and collision
            DIM yc(25) AS STATIC SINGLE     ' empirically determined
            DIM zc(25) AS STATIC SINGLE
            tog = %True
    END IF

    SELECT CASE vektor
           CASE 0
                  ARRAY DELETE xc(), @pDoppler.xac    ' circular buffer with acceleration data. Most recent data now in xc(last)
                  'calculate the shape:
                  xslope = (xslope + xc(0)) / 2       ' low pass filter - should cut off around 25Hz
                  xdown = (xdown + xc(25)) /2
                  IF (xslope > sens) AND (xdown < -sens) THEN       ' this is the pattern recognition condition
                           Gesture.collision(0) = xslope - xdown    ' always positive, since xdown is negative !
                           INCR Gesture.collision_dur(0)
                           Gesture.impact(0) =  ar(230)             ' further research required for optimum value in the array
                           RESET Gesture.theacol(0), Gesture.theacol_dur(0)
                  ELSEIF (xslope < -sens) AND (xdown > sens) THEN    ' condition for theatrical collision
                           Gesture.theacol(0) = xdown - xslope       ' always positive, since xslope is negative !
                           INCR Gesture.theacol_dur(0)
                           RESET Gesture.collision(0),  Gesture.collision_dur(0)
                           Gesture.impact(0) =  ar(230)
                  ELSE
```

```
                        RESET Gesture.collision(0), Gesture.theacol(0), Gesture.impact(0)
                        RESET Gesture.collision_dur(0), Gesture.theacol_dur(0)
                END IF
        CASE 1
                ARRAY DELETE yc(), @pDoppler.yac    ' the accelleration values are updated 256 times a second
                yslope = (yslope + yc(0)) / 2
                ydown = (ydown + yc(25)) / 2
                IF (yslope > sens) AND (ydown < -sens) THEN
                      Gesture.collision(1) = yslope - ydown
                      INCR Gesture.collision_dur(1)
                      Gesture.impact(1) = ar(230)
                      RESET Gesture.theacol(1), Gesture.theacol_dur(1)
                ELSEIF (yslope < -sens) AND (ydown > sens) THEN
                      Gesture.theacol(1) = ydown - yslope
                      Gesture.impact(1) =  ar(230)
                      INCR Gesture.theacol_dur(1)
                      RESET Gesture.collision(1),  Gesture.collision_dur(1)
                ELSE
                      RESET Gesture.collision(1), Gesture.theacol(1), Gesture.impact(1)
                      RESET Gesture.collision_dur(1), Gesture.theacol_dur(1)
                END IF
        CASE 2
                ARRAY DELETE zc(), @pDoppler.zac
                zslope = (zslope + zc(0)) / 2
                zdown = (zdown + zc(25)) / 2
                IF (zslope > sens) AND (zdown < -sens) THEN
                     Gesture.collision(2) = zslope - zdown
                     Gesture.impact(2) = ar(230)
                     INCR Gesture.collision_dur(2)
                     RESET Gesture.theacol(2), Gesture.theacol_dur(2)
                ELSEIF (zslope < -sens) AND (zdown > sens) THEN
                     Gesture.theacol(2) = zdown - zslope
                     Gesture.impact(2) =  ar(230)
                     INCR Gesture.theacol_dur(1)
                     RESET Gesture.collision(2),  Gesture.collision_dur(2)
                ELSE
                     RESET Gesture.collision(2), Gesture.theacol(2), Gesture.impact(2)
                     RESET Gesture.collision_dur(2), Gesture.theacol_dur(2)
               END IF
    END SELECT

    Gesture.collision(3) = MAX(Gesture.collision(0), Gesture.collision(1), Gesture.collision(2))
    Gesture.theacol(3) = MAX(Gesture.theacol(0), Gesture.theacol(1), Gesture.theacol(2))
    IF Gesture.collision(3) THEN
        Gesture.impact(3) = MAX(Gesture.impact(0), Gesture.impact(1), Gesture.impact(2))
    ELSEIF Gesture.theacol(3) THEN
        Gesture.impact(3) = MAX(Gesture.impact(0), Gesture.impact(1), Gesture.impact(2))
    ELSE
        RESET Gesture.impact(3)
    END IF

END SUB
```

Here is a plot of the result of the collision detection algorithm:

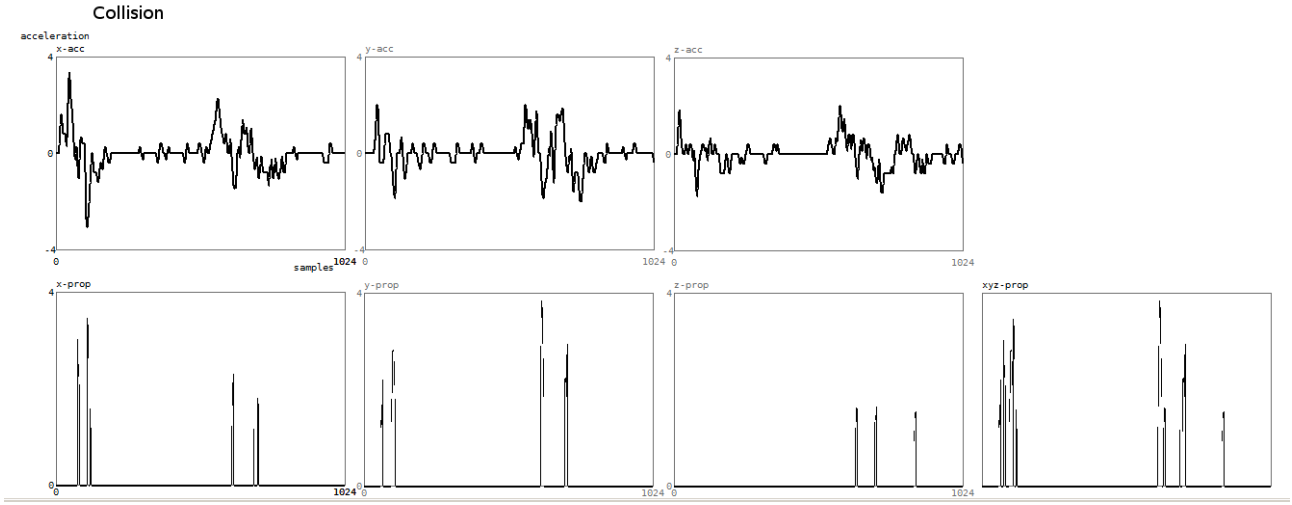

In this case the upper graphs show the vectorial acceleration channels. Theatrical collision detection resulted in the graphs below:

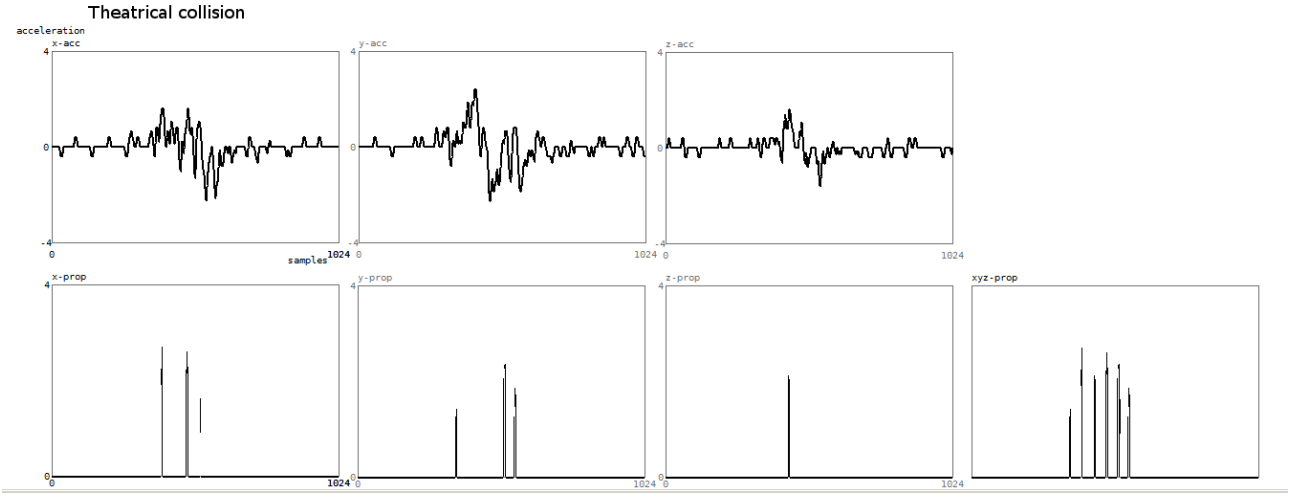

5. Roundness - Edginess

The spectral analysis of the Doppler signals in the short data buffer allow us to discriminate between gesture properties situated on a dipole that can be described as 'roundness' versus edginess. Other ways to describe the gesture characteristic referred to could be smooth and shaky or jagged.

definition: roundness applies if the gestures are smooth and continuous; edginess, if the gestures contain many abrupt components and discontinuities. The property reflects aspects of the shape of a gesture very well.
The analysis is based on the spectral power distribution in the fast data buffer (250ms). The code as we wrote it at first for the Fourier transforms is:

```
SUB DFT_Dbl (Samp#(), Sp#()) EXPORT

     'discrete fourier transform on double precision data
     LOCAL x, i, maat, halfsize AS LONG
     LOCAL kfaktor#, kt#, Rl#, Im#, g#, pw#
     DIM a(UBOUND(Samp#)) AS LOCAL DOUBLE
     maat = (UBOUND(Samp#)) + 1 ' must be a power of 2
     halfsize = maat / 2
     'note: size of Sp# must be Sp#(halfsize-1)
     kfaktor# = Pi2 / maat ' this is eqv. to ATN(1)* 8# / maat
     MAT a() = (1.0/maat) * Samp#()
     i = 0
     DO

          kt# = kfaktor# * i
          RESET Rl# , Im#
          FOR x = 0 TO maat - 1

               g# = (kt# * x)
               Rl# += (a(x) * COS(g#))
               Im# -= (a(x) * SIN(g#))

          NEXT x
          pw# = (Rl# * Rl#) + (Im# * Im#) ' sum of squares
```

```
            IF pw# THEN Sp#(i) = 2 * SQR(pw#)
            INCR i

        LOOP UNTIL i = halfsize ' the second half would be empty

    END SUB
```

In a later 10-fold improvement for speed, we recoded this using lookup tables for the sine and cosine factors and added the application of a Hanning window inline. The resulting code obviously becomes a lot less readable. All DFTs in our gesture recognition code are performed with a 25% overlap. To classify these properties, we split the power spectrum frequency bins in Sp#() in two parts at a variable point i. Note that our spectrum is 8 octaves wide (4 Hz to 512 Hz) and thus, taking into account the linear nature of the frequency distribution in the transform, we have to set i=15 for a normal midpoint at 64Hz. Then we sum up the power in the spectral bands up to i, as well as the power in the spectral bands i+1 up to the highest frequency. The power found in the lowest bin at Sp#((0) is dropped. If lw is the first sum, and hw the second, the smoothness property for each vector is calculated as 1 - (lh / (lw+lh)) and for the edgy property as 1 - (lw/(lw+lh)). The structure also returns the durations of these mutually exclusive properties in 1/256 s units. The algorithm for this property runs at a much lower speed of 16Hz, thus guaranteeing a data overlap of 25% on each refresh. Performing the required transforms much faster causes too much jitter in the behaviour of our real time multitasker. A consequence of this is that the durations are incremented in 16 unit steps (62.5 ms).

As we found that the analysis of the power spectrum offers a good basis for the analysis of some gestural features, we created a thread in the software to perform the spectral transforms on all three data buffers continuously. The results are returned to the user via pointers in the gesture structure: gesture.pspf() for the fast transform (4 Hz-512 Hz in 128 bands, with a refresh frequency of 25 Hz); gesture.pspm() for the medium buffer transform (1 Hz- 128 Hz in 128 bands, with a refresh frequency of 5 Hz), gesture.psps() for the slow buffer transform (0.25 Hz- 32 Hz in 128 bands, with a refresh frequency of 1.25 Hz).

6. 'Airborneness'

We came upon this gesture property when doing experiments with balls thrown through the sensor system. When looking into the spectral analysis data obtained, we noticed that for flying objects, the spectrum is discontinuous and reveals a gap on its low end. By looking at the size of the gap, we can distinguish flying objects – or for that matter, similarly, acrobatic jumps – from bodies in contact with the ground. The reason for this is quite easy to understand, if we realize that a moving body normally always has some parts at rest, even when extremities such as arms, legs, head are moving vehemently. The Doppler noise bands returned are therefore continuous and always start at zero. Airborneness might not be the most useful feature to extract from musicians' gestures, but forms an attractive bonus if it comes to dance movement analysis. It will be obvious that the time frame for this property detection has to be made very short and that the persistence values of the property cannot attain high values.

When coding for recognition of this property, one has to be very careful to take into account the spread of the background noise in the spectrum. To clarify this, we provide here a plot of the maxima encountered in the spectral transform over the 250ms time window (x-vector) without any body in the set-up:

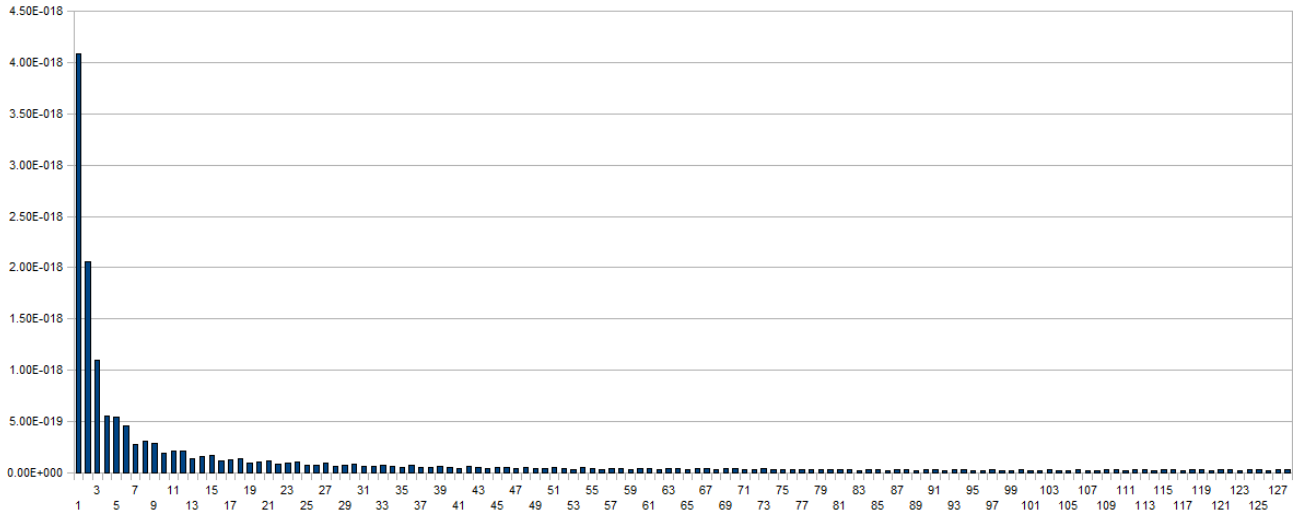

The values on the horizontal axis are the frequency bins and have to be multiplied by a factor of four to obtain real-world frequency values. The measurement time for this plot was 2 minutes. For proper evaluation of spectrum-based gesture properties, this basic noise spectrum has to be subtracted from the acquired data arrays. From a scientific point of view, the superior way of handling this would be by letting the software measure the basic noise spectrum on initialisation. Taking into account the stringent conditions for a meaningful measurement (no moving bodies or objects in the neighbourhood as well as a measurement time of a few minutes), we instead used a rough approximation of the curve in our coding. Here are two typical spectrum plots thus obtained during a jump:

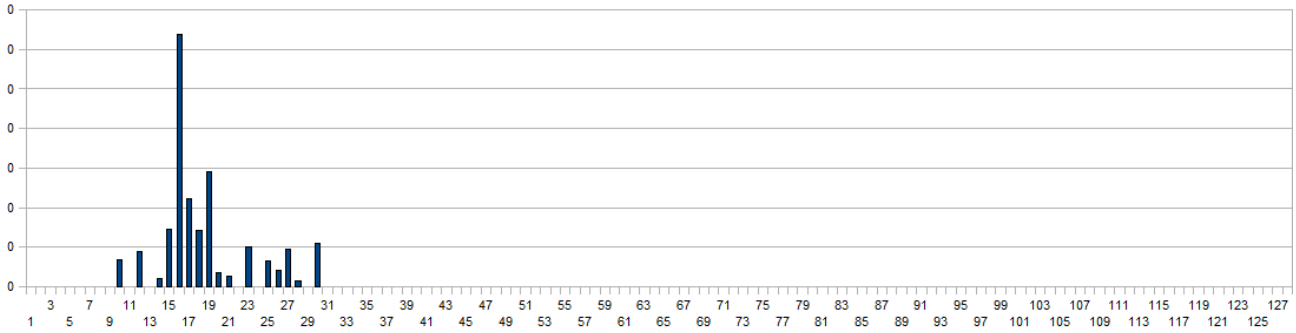

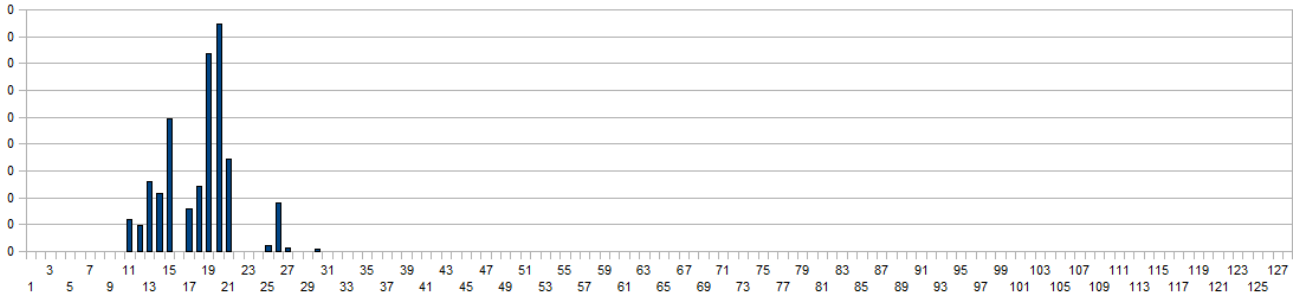

The vertical scaling was adapted to a factor of 10, to cope with the higher dynamic range obtained here. Unfortunately, due to the refresh speed limitations of the transforms in our coding, this property can only be calculated at a rate of 8 times a second. Hence, the duration field returns only a rough estimate of the time the body is airborne and cannot be used for precise measurement of jumps. However, the shape of the gesture during the jump is reflected pretty well in the spectrum obtained. In order to optimize the recognition code for speed, we converted the spectra to octave bands first. Then we evaluated the proportion of power distribution in the lowest two bands to the sum of all the higher bands. If the total power is higher than a measured noise level and this proportion exceeds an empirically determined value (a value of 17 was found), the property is set. The reliability of jump detection using this algorithm is higher than 90%.

7. Tempo and periodicity

The most difficult gesture property to retrieve in real time is periodicity. It represents a well known problem that has been treated in depth by a lot of different authors in very different contexts. The problem is the same whether applied to music or to gesture. We need information about periodicity in the gesture because it allows us the derive a tempo from gesture input.

There are a number of different algorithms possible, each with pros and cons. Since we are dealing with slow periodic phenomena, the fastest algorithm consists of measuring the time between periods (1/t equals frequency then) and checking the deviation from the mean on each new periodic phenomenon. The fastest algorithm starts from the collision detector, and yields a delay time in the order of 100ms. Synchronization is well possible, but latency and sudden jumps cannot be avoided. For clearly colliding periodic gestures, this method is very reliable and precise as long as the periodicity stays below 4 Hz (tempo MM240). However it imposes many restrictions on the type of gesture input. The jitter on the periodicity can be used as a base to calculate a fuzzy value for the tempo property. For the kind of gestures made by a conductor, we found that this path can be followed although the results are not always very convincing.
The FFT approach can be followed as well, but since it has to work on the 4 second buffers if it is to resolve tempi as low as MM30, the latency will be very large. The advantage is that it also works on less clear-cut gesture input. A serious disadvantage is that synchronizing with the input is difficult. The code as we wrote it, tries to cancel out the frequent occurrences of harmonics in the spectral transforms. Yet, it is far from perfect although we have been using it to synchronize music coded in midi files or calculated in real time with dancers on stage.

In the FFT approach, we coded a task that tries to derive a musical tempo expressed in MM numbers by interpolating between the frequency bins from the spectrum transforms. Here is a code snippet:

```
' spectra obtained after a DFT with a hanning window in the FFT thread
' vectors are 0,1,2 for the x,y,z buffers and 3 for the sum.
DIM sps(128) AS LOCAL DOUBLE AT @gesture.psps(vector)
i = ArrayMax_Dbl (sps()) 'find the strongest frequency bin
IF i THEN


        gesture.periodic(3) = ((i+1) * 15) - (7.5 * sps(i-1)/sps(i)) + (7.5 * sps(i+1)/sps(i))
        gesture.jitter(3) = (SQR(sps(i) + sps(i-1) + sps(i+1))) * 1E9


ELSE


        gesture.periodic(3) = 15 + (7.5 * sps(1)/sps(0))
        gesture.jitter(3) = (SQR(sps(0) + sps(1))) * 1E9


END IF
' now we try to evaluate the spectrum
RESET ct
FOR i = 0 TO 2


        IF ABS(gesture.periodic(i) - gesture.periodic(3)) < gesture.periodic(3)/ 20 THEN
```

```
                                                        ' 5% deviation allowed

                INCR ct

        ELSEIF ABS((gesture.periodic(i)/2) - gesture.periodic(3)) < gesture.periodic(3)/ 20
        THEN

                INCR ct 'in this case the i vector must be an octave above the sum of
                vectors

        ELSEIF ABS((gesture.periodic(i)*2) - gesture.periodic(3)) < gesture.periodic(3)/ 20
        THEN

                INCR ct 'in this case the i vector must be an octave below the sum of
                vectors

        ELSEIF ABS((gesture.periodic(i)/3) - gesture.periodic(3)) < gesture.periodic(3)/ 20
        THEN

                INCR ct 'in this case the i vector must be an fifth above the sum of
                vectors

        END IF

NEXT i
SELECT CASE ct

        CASE 0

                gesture.jitter(3) = gesture.jitter(3) ^4 ' no periodicity

        CASE 3 ' here we are certain, although we may have the wrong octave.

                gesture.jitter(3) = gesture.jitter(3) ^ 0.25

        CASE 2 ' high probability

                gesture.jitter(3) = gesture.jitter(3) ^ 0.5 ' we should see how the
                one deviating period relates to the equal ones.
                ' if it is a harmonic, we could increase confidence

        CASE 1

                gesture.jitter(3) = gesture.jitter(2) ^ 1.5 ' decrease certainty

END SELECT
```

A final approach, leading to quite reliable results under restricted conditions, although still with a fair amount of latency, makes use of cepstrum analysis. The usual method was followed here: starting from the power spectrum obtained on the slow data buffer, the log of the spectrum is calculated. On this dataset an inverse DFT is performed, yielding a series of periodicities defined in the time domain. In the literature these are referred to as 'quefrencies'. If this transform shows up a clear peak in the section after the initial impulse response burst, this peak is likely to correspond with a clear periodicity in the gesture. It will take time to investigate all the variants in coding and implementation, but all our results have been quite disappointing. Presumably the relatively high amount of simultaneously present non-periodic signal components in the input spectrum are at the origin of the failures. More sophisticated filtering techniques on the spectrum data prior to performing the cepstrum transform might be a remedy. However, even when we get it to work, synchronization with the input in real time remains very problematic and presumably can only be done if the calculated tempo is applied to an event taken from the fast data buffer. Suggestions for improved code and maths here are most welcome.

8. Freeze

A gesture property almost so trivial that we might almost forget to mention it: the absence of movement. We could also have named it rest, referring to the musical meaning. Absence of movement can be detected as soon as the received signals start sinking away into the noise floor. This happens when no body is in the set-up. A gesture freeze with a body in the field of the sensors will always have signal levels above absolute noise, since a living body always moves. Therefore, this property is not binary, but again a fuzzy value with a duration of its own.

A plot of input data versus analysis results is shown below. In this example, only the Y-vector has triggered the freeze property:

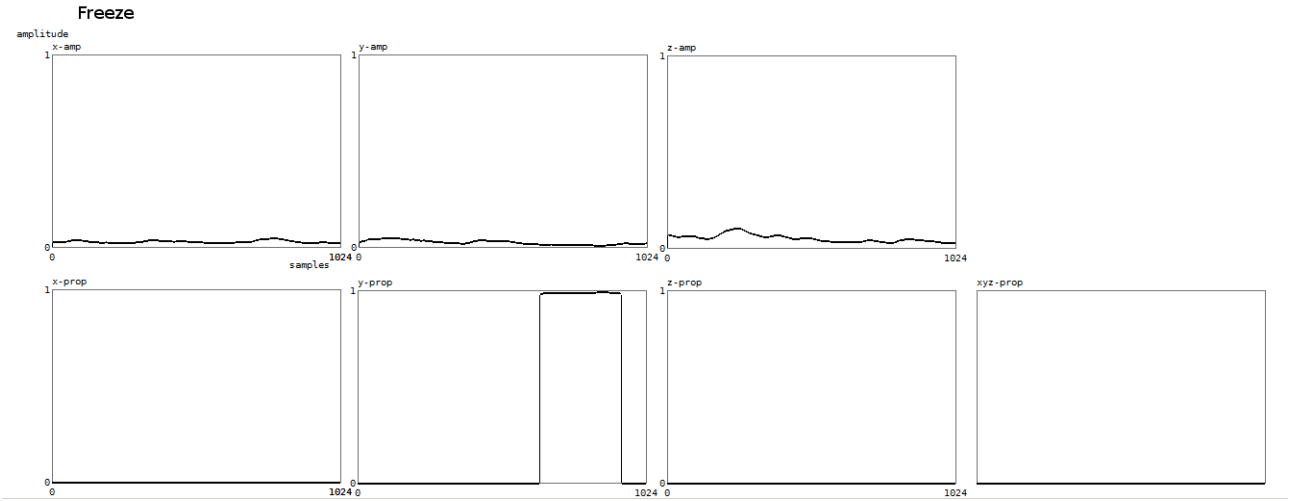

As of the time of the writing, the complete structure used to return our gesture properties to the user looks like:

```
TYPE GestureType DWORD
     collision (3) AS SINGLE         '0=X, 1=Y, 2=Z, 3= total     acceleration based, the values are the correlation magnitude
     collision_dur (3) AS LONG       'in 1/256 s units
     theacol   (3) AS SINGLE         'theatrical collision        acceleration based
     theacol_dur (3) AS LONG         'in 1/256 s units
     implo     (3) AS SINGLE         'surface based  - normalized property strength
     implo_dur (3) AS LONG           'in 1/256 s units 0 at the start of detection, climbing up as long as the property is valid.
     implo_val (3) AS SINGLE
     explo     (3) AS SINGLE         'surface based  - normalized property strength
     explo_dur (3) AS LONG           'duration of the property in 1/256 s units
     explo_val (3) AS SINGLE         'prediction value of the property (FIR output)
     speedup   (3) AS SINGLE         'speed based
     speedup_dur (3) AS LONG
     speedup_val (3) AS SINGLE
     slowdown  (3) AS SINGLE         'speed based
     slowdown_dur (3) AS LONG
     slowdown_val (3) AS SINGLE
     periodic  (3) AS SINGLE      'should give the tempo in MM units
     jitter    (3) AS SINGLE      'should give the degree of certainty of the above tempo.
     flue      (3) AS SINGLE      'gives the standard deviation for the surface buffer  (in fact 1-s)
                                  ' constant body surface property
     flue_val  (3) AS SINGLE      'gives the average value for the surface buffer   (normalized 0-1)    size of body surface
     flue_dur  (3) AS LONG        'duration in 1/256 s units
     fixspeed  (3) AS SINGLE      'speed based, gives standard deviation for the frequency buffer
     fixspeed_val (3) AS SINGLE   'gives the average value of the constant speed
     fixspeed_dur (3) AS LONG     'duration in 1/256 s units
     impact    (3) AS SINGLE      'surface of the body on the moment of detected collision (not a gesture property!)
     smooth    (3) As SINGLE
     smooth_dur(3) AS LONG
     edgy      (3) AS SINGLE
     edgy_dur  (3) AS LONG
     airborne (3) AS SINGLE
     airborne_dur (3) AS LONG
     freeze    (3) AS SINGLE      'property set when no movement is detected above the noise level
     freeze_dur (3) AS LONG       'in 1/256 s units
     freeze_val (3) AS SINGLE     'normally = 1- freeze, value always set
     distance  (3) AS SINGLE      'requires the combination of radar and sonar.
     pspf (3) AS DOUBLE  PTR          'pointer to the spectral transform data for the fast buffer
     pspm(3) AS DOUBLE PTR            'pointer to the spectral transform data for the medium buffer
     psps(3) AS DOUBLE PTR            'pointer to the spectral transform data for the slow buffer
     algo              AS DWORD       'parameter for algorithm to use (for research)
     Sorder            AS DWORD       'FIR filter order for the surface related properties
```

```
    Forder            AS DWORD      'FIR filter order for the speed related properties
END TYPE
```

Since the entire structure is recalculated 256 times a second, responsiveness is pretty good, certainly in comparison with competing non-radar or sonar based technologies. We performed some measurements to estimate the processor load and found out that the complete gesture analysing procedure takes between 12 MIPS and 25 MIPS, using a quad core Pentium processor. That is about half of the available capacity. More than half of this processor load is due to the spectral transforms. The full source code as well as compiled libraries (DLLs) are available from the author for evaluation. The software, with slight modifications, can also be used without the National Instruments data acquisition device (4) , if a decent quality four channel sound card is used. We have sensors available that can connect directly to audio inputs of a PC. These do not require a analogue computing and processing board. We welcome contributions from other researchers and invite them to use, test and improve our approach.

dr.Godfried-Willem Raes

Notes:

(1) Thanks to my dance and music collaborators who helped me perform the many necessary experiments and measurements using their bodies: Moniek Darge, Angela Rawlings, Helen White, Dominica Eyckmans, Lazara Rosell Albear, Zam Ebale, Marian De Schryver, Nicoletta Brachini, Emilie De Vlam, Tadashi Endo, Nan Ping, Jin Hyun Kim and many others. Thanks also to my collaborator Kristof Lauwers to help out with code development, data analysis and debugging.

(2) All our code is written in PowerBasic and compiled with their Windows compiler, version 9.04. The code is part of a fairly large programming environment that we have developed for real time composition: GMT. We have put it in the public domain and all source code is available on the Logos website.

(3) Namuda is a word of our own invention, derived from 'naked music dance.' We felt the need for a new word to describe the very dance-related method of music-making entailed by the development of our invisible instrument.

(4) A big advantage to using the National Instruments devices is that they are per definition very well supported in Labview, undeniably the leader in professional instrumentation software and tools for analysis.

Bibliographical references:

- BECKMANN, Petr & SPIZZICHINO, Andre "The Scattering of Electromagnetic Waves from Rough Surfaces", Pergamon Press, Oxford, 1963
- DROITCOUR, Amy Diane "Non contact measurement of hearth and respiration rates with a single-chip microwave doppler radar", Stanford PhD thesis, June 2006.
- RAES, Godfried-Willem "Een onzichtbaar muziekinstrument" (Gent, 1993, Ph.D. thesis)
- RAES, Godfried-Willem "An Invisible Instrument (1994)
- RAES, Godfried-Willem "Gesture controlled virtual musical instrument" (Ghent, 1999)
- RAES, Godfried-Willem "Quadrada" (Ghent, 2003)
- RAES, Godfried-Willem "PicRadar" (Ghent, 2004-2005)
- RAES, Godfried-Willem "Distance sensing devices" (Ghent, 2007)
- RAES, Godfried-Willem "Microwave Gesture Sensing"(Ghent, 2009)
- RAES, Godfried-Willem "Holosound 2010, a doppler sonar based 3-D gesture measurement system " (Ghent, 2010)
- ROADS, Curtis “The computer music tutorial”, (MIT press, 1996)

First sketch of this chapter published on the web: 05.05.2010 by Dr. Godfried-Willem Raes.

3

<Namuda>

by
Dr. Godfried-Willem Raes

post-doctoral researcher
Ghent University College & Logos Foundation

2010

This paper describes the application layer for gesture recognition using Doppler-based hardware systems. For a good understanding it is advised that readers familiarize themselves first with the hardware described in "Holosound 2010, a doppler sonar based 3-D gesture measurement system" as well as with our paper on namuda gesture recognition. This paper is the last part of a triptych covering the namuda dance project developed at the Logos Foundation (1). Namuda is a word of our own invention, derived from 'naked music dance.' We felt the need for a new word to describe the very dance-related method of music-making entailed by the development of our invisible instrument.

Being capable of recognizing a defined set of gestures in a piece of software is of little significance if an application layer fails. Namuda dance technique requires a mutual adaptation of the performer and the software parameters. In order to make the study of namuda dance possible, we have designed a series of études in which a single gesture prototype can be practised. Since visual feedback to the performer is very problematic in the context of performance, for it greatly hinders freedom of movement and is by nature too slow, we have opted for auditory display. The robot orchestra (2) as we have designed and built it, makes a good platform for such auditory display, particularly since the sounds are not virtual (loudspeakers) but real acoustic sounds emanating from real physical objects. In fact just about any musical instrument can be seen as an example for auditory display as it by its very nature truthfully converts a certain subset of fine motor skills and gestures into sound. The gestures underlying music practice may very well constitute a basis for the embodiment underlying the intelligibility of music. (3) The motor skills and gestures entailed by the playing traditional musical instruments is obviously instrumental in nature. It is dictated by the mechanical construction of the instrument. Therefore, as an extension of the body, an instrument can, at most, be a good prosthesis. By removing the necessity of a physical object, the body becomes the instrument. But this in no way removes the necessity of motor skill and gestural control.

1. Namuda études

The scheme followed for each étude is always the same: starting with the default parameter settings

in the software, the performer has to practice each gesture prototype until the recognition is optimum, as can be judged from the response of the robots. The default parameters are not arbitrary, but have been determined as a result of hundredths of measurement sessions with about twenty different subjects, male and female. Each gesture prototype is mapped to a different subset of responding robots. In this respect the study of namuda gestures is quite similar to the study of any musical instrument. A certain level of fine motor control has to be developed in the player. Only once that level has been reached can the recognition software be modified by changing the parameters slightly. One would never buy a new and better violin for a child, every time it makes a handling and playing mistake. Only once it knows the basics reasonably well should buying a better instrument become an option. Fortunately, in the case of the invisible instrument, we do not have to buy a new instrument but we can improve the software and adapt it to the player. This last possibility opens a whole new perspective for future developments in instrument building.

1.1: Speedup

To study steady accelerating movements, we made a mapping on the x, y and z vectors for the oboe (<Ob> robot), the cornet (<Korn> robot) and the saxophone (<Autosax> robot) respectively. The speedup property strength is mapped on the pitch the instruments will sound whereas the sound level is controlled by the value of the speed parameter. It is a good exercise to try to have the instruments play as long as possible by stretching the time over which the property can remain in a set state. As soon as the property is set in all three vectors, the large stainless steel shells that make up <Llor> will come into play. The sensitivity is set at a much lower level for this to happen than is the case for the vectors taken separately.

1.2: Slowdown

The slowdown property can obviously only be set when the starting gesture is in movement already. Thus the property can never be triggered from rest. The étude maps all three vectors on pitches in the <Piperola> and <Bourdonola> robots. These are flue pipe organs. The pitch depends on the value of the slowdown, not on the property strength. When the property is set in all three vectors, the lights on the piperola robot will flash.

1.3: Fixspeed

This property gets set as soon as detected speed of a movement stays reasonably constant within a timeframe of 500 ms. It is pretty difficult at first to trigger this property more than just accidentally. The reason is not only due to our control, but also in part due to the cosine factors on the doppler frequency shifts. The latter can be much improved and even cancelled out by keeping the angle of the movement axis and the sight of the vectorial transducer constant.
The mapping of all three vectors here is on one of our smallest robots: <Toypi>, an automated toy piano. When all three vectors have the property set, the lights on the little robot come up.

1.4: Expanding

To trigger this property a movement is required whereby the amount of moving body surface gradually is increased. Associate the property with growth, explosion, enlargement. The property can be triggered from a standstill.
The x-vector is mapped on our <Klung> robot, an automated Indonesian anklung with brass chimes. Pitch selection is mapped on property strength whereas volume is

correlated to the value of the property. The y-vector similarly is mapped on <Simba>, a cymbal playing robot. The z-vector is mapped on <Springer>, a somewhat hybrid robot combining shakers, very large springs mounted on resonators as well as a big motor driven siren. The selection of the elements playing in this robot is mapped on the duration of the property in the Z-vector.
When all three vectors are set, the lights on the <Simba> robot will come up.

1.5: Shrinking

Being the other side of the dipole to the previous property, the gestural associations can also be formulated as imploding, diminishing, getting smaller. Clearly the property presupposes movement to start from.
The mapping is as follows: x-vector on <Xy>, a quarter tone xylophone robot; y-vector on <Tubi>, a quarter tone robot made with thick aluminium tubes; z-vector on <Vibi>, an automated vibraphone. For all three vectors, property strength is mapped on the pitch and property value on the sound level. When the property is triggered in all three vectors the lights on <Xy> will flash.

1.6: Steady

In order to trigger this property it is required that the amount of body surface in movement remains constant within the time frame of measurement. The mapping for this property is on our quarter tone organ robot <Qt>. When the property is set in all three vectors, the blue lights on the robot will come on. In this mapping the amount of body surface remaining constant determines the pitches of the notes. The attack velocity of the notes is controlled – in a rather subtle way – by the property strength.

1.7: Smooth
1.8: Edgy

These gesture prototypes can be practised together. The edgy property-strength is mapped to the piano notes, played by our player piano robot. The smooth property is mapped to the pitches of our quarter tone organ robot, <Qt>. The attack velocity is controlled by the momentary value of the vectorial moving body surface. The property is set based on an analysis of the spectrum of the Doppler signals. Edgy movement with many sudden changes causes an overweight of higher partials in the spectrum. The sound volume from Qt is made to be a (slow) function of the value of the low side of the power spectrum. It had to be slow reacting for it steers the compressor on the organ. Those motors, due to their inertia, cannot change speed suddenly. The recognition quality was rated as excellent by all performers we have subjected to this étude so far.

1.9: Freeze

To practice this 'non-gesture', we applied an inverse mapping, whereby sound will be heard as long as the freeze property is not triggered. The robot used in this mapping is <Bourdonola>, a low register open organ pipes with a string-like sound. The étude is very fundamental as it lets the performers experience the very high sensitivity level of the system.

1.10: Jump

The airborne gesture property is set when the performer jumps and no part of the body

is at rest. False triggering can occur on large stepping movements though. The larger or higher the jump the stronger the property will be defined. For this étude the x, y and z-vectors are respectively mapped to <Heli> (a helicon robot) <Bono> (a trombone robot) and <So> (the sousaphone robot). When the property is defined for all three vectors, both castanet-playing robots will join. The sound volume is mapped on the amount of body mass involved whereas the pitch will be proportional to the property strength.
When all three vectors have the airborne property set, certainty is nearly 100%. If only two vectors trigger the property, certainty is still higher than 90%. Most often it is the Z-vector that fails to trigger, which is easily explainable by the fact that the transducer for that vector is suspended above the performer. In order to be certain that the Z-vector also triggers the property, the jump must also include a positional displacement. Needless to add, this étude is quite exhausting to perform.

1.11: Collision

Determination of this gesture property being based on acceleration followed by a sudden stop, it implies a well-defined sudden stop in the gesture. Rebounding movements should be avoided as they can result in false or double triggering. To make the étude convincing, we mapped the output to nothing but percussion, the collision based instrument par excellence. The étude should be performed using all possible parts of the body: not only arms and legs, but also the head, the entire torso, the feet, the elbows and even the belly if musculature allows it...
The x-vector is mapped to the drums in <Troms> (a set of drums) and the <Snar> robot, an automated snare drum. The y-vector is mapped to the the cowbells that make up the <Vacca> robot. The z-vector is mapped to the set of woodblocks in the <Thunderwood> robot as well as to the thin metal sheets in the <Psch> robot. When collision is detected in all three vectors, the cymbal in the <Troms> robot will play. If collisions are detected but they are below the sensitivity level set in the software, the white lights on the robots will flash.

1.12: Theatrical Collision

As this prototype is defined as a decelerating movement ending in a stop and accelerating again – avoidance of real collision – it tends to be set more easily over relatively larger time spans. In our étude we mapped the gesture to our <Puff> robot, a percussive organ-like instrument tuned in quarter tones.

1.13: Periodic

This is the least well-functioning property in our set and it definitely needs further improvement. Response time is too slow and false triggers do occur regularly. The mapping on the drums in our <Troms> robot allows practice and evaluation. We have also developed software allowing performers to synchronize midi or audio file playback with gestural input. Within strict limitations such as no sudden tempo changes, avoidance of rhythmical complexities (doublings and triplets) it can even be got to work. Further research is being done based on cepstrum analysis.

Parallel to these recognition-based gesture properties, the implementation also offers a full set of very direct mappings of movement parameters on sound output:

- moving body surface: The most intuitive mapping for this parameter seems to be to sound volume or density.
- speed of movement: The most intuitive mapping for this parameter seems to be to pitch.
- spectral shape of the movement: The most intuitive mapping for this complex parameter seems to be to harmony.
- acceleration of the movement: The most intuitive mapping for this parameter seems to be to percussive triggers.

Of course there is nothing mandatory in the way the mappings of gestural prototypes have been laid out in these études. It is pretty easy to devise mappings more suitable for use out of the context of our own robot orchestra. The simplest alternative implementations consist of mappings on any kind if MIDI synth or sampler. But, mapping the data from our gesture recognition system to real time audio streams (as we did in our 'Songbook' in 1995, based on human voice sound modulation via gesture), is an even better alternative.

2. Extending the time frame

The gesture prototypes practised in the études reflect a gestural microscale in the time domain. Their validity may be as short as 7ms and can for most properties seldom exceed 2 seconds. The only gesture properties that can persist over longer time spans are freeze, periodic, edgy, smooth, fluent and fixspeed. Some can, by their nature, only be defined over very short time intervals: airborne and collision. These gesture prototypes are to be compared to what phonemes are in spoken language, although they already carry more meaning than their linguistic counterparts. Meaning here being understood as embodied meaning.

By following assignment and persistence of the gesture prototypes over longer time spans, say between 500 ms and 5 seconds, it becomes possible to assign expressive meanings to gestural utterances. Here we enter the level of words and short sentences, to continue using linguistic terminology as a metaphor. When we ask a performer to make gentle movements in order to express sympathy, then the statistical frequency of a limited subset of gesture properties will go up significantly. When we ask for aggression, the distribution will be completely different.

It is on this level of time scale, that quite a few of our gestural prototypes may be correlated to the classifications of 'effort' set up by Rudolf Laban in his text 'Effort ; Rhythmic Control of Man's activities in Work and Play'. This text was written well before 1950 and only got published as an appendix to the book mentioned in the bibliography of our paper. (Laban, 1980). As far as we can judge, his classification and notation proposals are difficult to hold in a more generalized context of a theory of expressive gesture. Clearly none of Laban's analysis are based on any other objective measurement than visual observation and the dancers' own experience of effort.

It would be an interesting research project to find out how comparable such distributions for a limited set of sentic forms (4) are amongst a large set of different dancers and musicians. Unfortunately this is beyond the scope of our own mission. In part, such research is being done now by our colleague Dr. Jin Hyun Kim.

3. Relation to other dance practices.

Although as soon as we gained some insight in the potential for dance offered by our technology – that was in the mid nineteen-seventies – we carried out artistic experiments with dancers trained in classical ballet as well as modern dance, we quickly found out that such an approach to dance was unsuitable to work well with this technology. Classical dance forms concentrate on elegance and – in general – in avoid collision and mass. Position in space and visual aspects are very dominant. Immediately alternative dance practices came into consideration. In the first place butoh dance, an

avant-garde dance practice with its roots in Japan, where we also came in contact with it (Through Tari Ito). Thus we got in contact with dancers such as Min Tanaka, Tadashi Endo, Emilie De Vlam and later on Lazara Rosell Albear ... This has led to quite a considerable list of collaborative performances. However, butoh from a technical dance point of view is only vaguely defined. Its non-avoidance of roughness, its nakedness (5) and its concentration on bodily expression, leaving out any distracting props and requisites, formed the strongest points of attraction. Only in some forms of contact improvisation did we find other links, but in this dance form we ran into problems with our technology, which is not capable of distinguishing the movements of more than a single moving body at the same time. As far as couple dances go, we also investigated tango (and the related milonga) quite a bit, in part also because we happen to be a tanguero ourselves. In this type of dance the problem of the two inseparable bodies poses less of a problem since movements are always very well coordinated. Acrobatic tango is of particular interest for the gestures used are very well defined. However, good dance couples in this genre are pretty rare. Moreover, acrobatic tango is generally highly choreographed, leaving little space for improvisation, thus not lending itself so well to genuinely interactive applications.

Other dance forms we have experimented with include pole dance, flamenco and break dance. For the first dance style, we even developed a special set of microwave radar sensors that can be mounted at the top of the pole. Unfortunately we found out that the professionals in this dance form have little if any affinity with the art forms we are interested in ourselves, which are after all still quite experimental. As for break dance we mus,t state that despite the fascination we have for the virtuosity in movement that can be found in the genre, it seems to be strongly bound to a certain age group that we have long since left behind us...

Although not normally thought of as a dance forms, movement practices as can be found in some sports and martial arts, seem to offer a good technical introduction to the namuda gestures considered here: karate and to a lesser extent judo. Karate is of a particular interest here because is exploits in full the development of very fast accelerating gestures.

4. Interactive composition and choreography

It will be clear that the mastering of namuda opens wide perspectives for the development of real time interactive composition with a strong theatrical component. Over the 35 years that we have been developing the system, many hundreds of performances have been staged. Here is a short overview of our own main artistic productions in which the technologies described here were developed and/or applied:

- Holosound (1980)
    - This was the first large scale music theatre performance using the purely analogue version of my invisible instrument. The performer was invariably Moniek Darge and the piece was performed at least 200 times all over the world. An alternative version functioning as an audio art installation was realized as well. A copy of the installation was purchased by the Museum of Musical Instruments in Brussels.
- A Book of Moves (1992)
    - This was the first large-scale composition using our invisible instrument. Each section of the piece demonstrates another way of directly mapping gesture derived parameters to sound generated by an assembly of samplers and synthesizers. The piece was performed over 350 times all over the world by the Logos Duo (the author and Moniek Darge). Together with the Holosound installation, the hardware and software for this production, is also available at the Brussels Museum of Musical Instruments. Another copy was purchased by 'het Muziekgebouw' in Amsterdam, where it is part of their sound garden.
- Songbook (1995)

        - In this full evening production we used our invisible instrument to control the sounds of the performers' voices in real time through pure wireless gesture commands. Thus gesture-controlled pitch shifting, a variety of effects, harmonizers and filters as well as the build-up of a large choir from a single voice, were implemented and demonstrated. The piece makes use of a bank of DSP sound processors. It has been performed over a hundred times all over the world. Performers have been Moniek Darge, Karin Defleyt, Joachim Brackx and the author.
- Gestrobo Studies (2000)
    - This is the first collection of pieces using the sonar-based invisible instrument as well as the robot orchestra. Different sections of the suite were performed many times by performers Emilie De Vlam, Tadashi Endo, Marian Deschryver, Nicoletta Branchini, Dominica Eyckmans and others.
- Quadrada Studies (2001)
    - The first collection of pieces using the microwave radar-based version of the invisible instrument with mappings to the robot orchestra. Performers of different pieces in this suite have been: Angela Rawlings, Helen White, Moniek Darge and Nicoletta Branchini.
- TechnoFaustus (1998-...)
    - Although try-outs of many different acts in this large scale opera project have been presented throughout our regular concerts, the full production as yet still awaits its premiere. The try-out acts have been performed by Moniek Darge, Emilie De Vlam, Kristof Lauwers and the author.
- Hanaretemo (2009)
    - A full evening music theatre production using almost all of the technologies we have hitherto developed for gesture sensing. It was performed by Emilie De Vlam and Nan Ping as butoh dancers.
- Namuda Studies (2010-)
    - Being the most recent development in our artistic production it remains as yet unfinished. Nevertheless we present new contributions to the collection on a very regular basis at our concerts with the robot orchestra. Performers are Emilie De Vlam, Zam Ebale, Lazara Rosell Albear and Dominica Eyckmans and we hope to extend the number of performers willing to undertake some training in namuda mastership.

The entire namuda system including the invisible instrument is open for use by other composers and performers. Scientists interested in research into human gesture are also invited to explore the possibilities of the system. Other composers that have made use of it so far are Kristof Lauwers and Yvan Vander Sanden. The system has also been investigated by Hans Roels, Troy Rogers, Jin Hyun Kim, Dirk Moelants and others. Many applications have been developed on other platforms than our own GMT-programming environment. To facilitate this, we have designed a limited gesture sensor with built-in signal processing using a PIC micro-controller. This 'Picradar' sensor, as we baptized it, makes use of microwave radar (9.35 GHz) and outputs its data following the midi protocol. (6) It can readily be used in PD, available for the PC, for Linux and even running on a Mac.
There is still a lot of work left to be done on improvements to the hardware and recognition software as well as in terms of its artistic implementations. An open invitation.

Dr. Godfried-Willem Raes
Ghent, May 2010

Notes:

(1) Thanks to my dance and music collaborators who helped me perform the many necessary experiments and measurements using their bodies: Moniek Darge, Angela Rawlings, Helen White, Dominica Eyckmans, Lazara Rosell Albear, Zam Ebale, Marian De Schryver, Nicoletta Branchini, Emilie De Vlam, Tadashi Endo, Nan Ping, Jin Hyun Kim and many others. Thanks also to our collaborator Kristof Lauwers to help out with code development, data analysis and debugging. Last but not least, thanks to the Ghent University College that succeeded in freeing us from teaching tasks such that we were given plenty of support to conduct our research.

(2) Detailed information on the robot orchestra and the robots constituting it can be found at http://www.logosfoundation.org/instrum_god/manual.html

(3) These matters were discussed in depth in my texts on the invisible instrument: Raes,1993 ,1994 and 1999.

(4) The notion of sentic forms was introduced by Dr. Manfred Clynes, with whom we had many conversations and discussions at the time we visited him in Sydney when we were demonstrating our invisible instrument at the Sydney Conservatory. References to his publications on the subject can be found in the bibliography section of this paper.

(5) We wrote an essay on nakedness some time ago, after realizing that even nowadays there are still people around that seem to have difficulty in coping with this utmost human property... The text can be read at : "Naked"

(6) A paper describing the Picradar project as well as some of its applications can be found at: http://www.logosfoundation.org/ii/picradar.html

Bibliographical references:

- CLYNES, Manfred "Sentics, the touch of the emotions" , Anchor Books (NY, 1978)
- KRAMER, Gregory (ed.) "Auditory Display", Addison-Wesley Publishing Company, (Reading MA, 1994)
- LABAN, Rudolf "The mastery of movement", Macdonald & Evans Ltd (Plymouth, 1980)
- RAES, Godfried-Willem "Een onzichtbaar muziekinstrument" (Gent, 1993, Ph.D. thesis)
- RAES, Godfried-Willem "An Invisible Instrument (1994)
- RAES, Godfried-Willem "Gesture controlled virtual musical instrument" (Ghent, 1999)
- RAES, Godfried-Willem "Quadrada" (Ghent, 2003)
- RAES, Godfried-Willem "PicRadar" (Ghent, 2004-2005)
- RAES, Godfried-Willem "Distance sensing devices" (Ghent, 2007)
- RAES, Godfried-Willem "Naked" (Ghent, 2008)
- RAES, Godfried-Willem "Microwave Gesture Sensing"(Ghent, 2009)
- RAES, Godfried-Willem "Holosound 2010, a doppler sonar based 3-D gesture measurement system " (Ghent, 2010)
- RAES, Godfried-Willem “Namuda Studies” [http://www.logosfoundation.org/scores_gwr/Namuda_Links/namuda_studies.html] (Ghent, 2010)
- ROELS, Jetty(ed.) "Images of corporeality, traces of Butoh in Flanders", VCIT, (Ghent, 2002)
- SEIFERT, Uwe, HYUN KIM, Jin (eds) "Paradoxes of Interactivity", (Bielefeld, 2008)
- TECK, Katerine "Movement to Music", Greenwood Press (Westport CT, 1990)

Last update:2010-09-10